

# Chiral-Extended Photon-Emitter Dressed States in Non-Hermitian Topological Baths

Zhao-Fan Cai,<sup>1,\*</sup> Xin Wang,<sup>2,\*</sup> Zi-Xuan Liang,<sup>1</sup> Tao Liu,<sup>1,†</sup> and Franco Nori<sup>3,4,5</sup>

<sup>1</sup>*School of Physics and Optoelectronics, South China University of Technology, Guangzhou 510640, China*

<sup>2</sup>*Institute of Theoretical Physics, School of Physics, Xi'an Jiaotong University, Xi'an 710049, China*

<sup>3</sup>*Theoretical Quantum Physics Laboratory, Cluster for Pioneering Research, RIKEN, Wakoshi, Saitama 351-0198, Japan*

<sup>4</sup>*Center for Quantum Computing, RIKEN, Wakoshi, Saitama 351-0198, Japan*

<sup>5</sup>*Department of Physics, University of Michigan, Ann Arbor, Michigan 48109-1040, USA*  
(Dated: August 23, 2024)

The interplay of quantum emitters and non-Hermitian structured baths has received increasing attentions in recent years. Here, we predict unconventional quantum optical behaviors of quantum emitters coupled to a non-Hermitian topological bath, which is realized in a 1D Su-Schrieffer–Heeger photonic chain subjected to nonlocal dissipation. In addition to the Hermitian-like chiral bound states in the middle line gap and skin-mode-like hidden bound states inside the point gap, we identify peculiar in-gap chiral and extended photon-emitter dressed states. This is due to the competition of topological-edge localization and non-Hermitian skin-mode localization in combination with the non-Bloch bulk-boundary correspondence. Furthermore, when two emitters are coupled to the same bath, such in-gap dressed states can mediate the nonreciprocal long-range emitter-emitter interactions, with the interaction range limited only by the dissipation of the bath. Our work opens the door to further study rich quantum optical phenomena and exotic many-body physics utilizing quantum emitters coupled to non-Hermitian topological baths.

*Introduction.*—Recent years have witnessed considerable interest in controlling photon-emitter interactions utilizing structured nanophotonic environments due to their potential applications in quantum networks and quantum simulation of many-body physics [1–23]. Among them, one of the promising strategies is to couple quantum emitters with topological waveguides [7–16], where the topological nature of the bath can give rise to unconventional quantum optical phenomena robustness against disorder, e.g., chiral photon-emitter bound states, band topology-dependent super/subradiant states, and exotic many-body phases resulting from the tunable emitter-emitter interactions mediated by the bound states [12].

A photonic structure is unavoidably coupled to the external reservoir, which can be effectively described by non-Hermitian Hamiltonians [24]. Non-Hermitian physics is currently a burgeoning field due to the unique physical phenomenon without Hermitian counterparts [24–69]. An intriguing physical phenomenon is the non-Hermitian skin effect (NHSE), with the emergence of localized bulk modes at boundaries [34–39], which has the intrinsic topological origin associated to the point gap [47, 52]. In recent years, the interplay of quantum emitters and non-Hermitian structured baths has attracted much attention [70–74], leading to exotic quantum optical behaviors, e.g. skin-mode-like bound state inside the point-gap loop and anomalous quantum emitter dynamics without Hermitian counterparts [72].

In this work, we predict the unique photon-emitter dressed states and long-range emitter-emitter interaction by studying a paradigm of photon-emitter interactions in a nonreciprocal Su-Schrieffer–Heeger (SSH) photonic chain. In addition to the existence of conventional chiral

bound states and hidden bound states inside the line and point gaps, respectively, we unveil unusual chiral and extended photon-emitter dressed states without Hermitian counterparts. Moreover, we demonstrate the directional long-range emitter-emitter interaction mediated by dressed states, where the interaction range is limited only by the bath dissipation.

*Model.*—We consider a set of  $N$  identical atoms, as quantum emitters, coupled to a 1D SSH photonic chain with  $L$  unit cells, as shown in Fig. 1. Each two-level atom, with ground state  $|g\rangle$  and excited state  $|e\rangle$ , is coupled to each cavity in the lattice, and its decay rate is denoted by  $\gamma$ . The SSH photonic chain consists of coupled cavities subject to an engineered nonlocal photon dissipation between two sublattices  $a$  and  $b$  in each unit cell with loss rate  $\kappa$ . In the single-excitation subspace, the system dynamics is governed by the effective non-Hermitian Hamiltonian (see details in the Supplemental Material

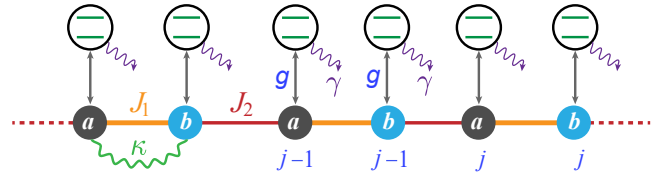


FIG. 1. Schematic showing a set of  $N$  identical two-level atoms (acting as quantum emitters) coupled to a 1D SSH photonic bath. The bath consists of coupled cavities, subject to correlated photon decay (with loss rate  $\kappa$ ) between two cavities in each unit cell.  $J_1$  and  $J_2$  denote the intracell and intercell hopping strength,  $\gamma$  is the atomic decay rate, and  $g$  is the atom-photon coupling strength.

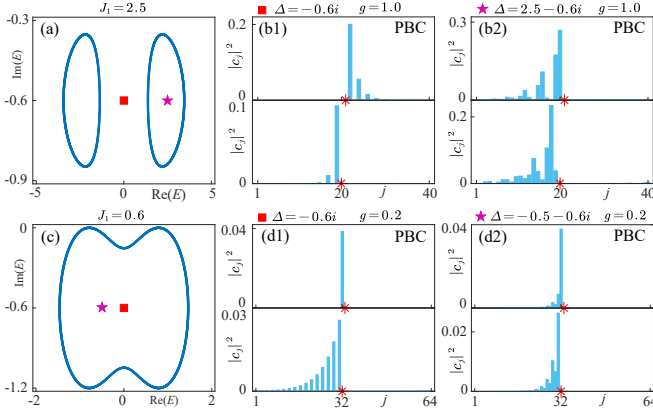


FIG. 2. Single-excitation spectrum (blue loops) under PBCs (a) with the coexistence of point and line gaps for  $J_1 = 2.5$ , and (c) with only a point gap for  $J_1 = 0.6$ . The markers denote the eigenenergies of the bound states of a single emitter coupled to the bath for different  $\Delta$ . The corresponding site-resolved photon weights  $|c_j|^2$  are shown in (b1,b2) and (d1,d2), where the emitter is coupled to the sublattice  $a$  (b), denoted by the red asterisk, for the top (bottom) plot. The other parameters used are  $\kappa = 1.2$  and  $J_2 = 1.0$ .

(SM) in Ref. [75])

$$\begin{aligned}
\hat{H}_{\text{eff}} = & \sum_{n=1}^N \Delta \hat{\sigma}_n^+ \hat{\sigma}_n^- + \sum_{j=1}^{L-1} J_2 (\hat{a}_{j+1}^\dagger \hat{b}_j + \hat{b}_j^\dagger \hat{a}_{j+1}) \\
& + \sum_{j=1}^L \left[ \left( J_1 + \frac{\kappa}{2} \right) \hat{b}_j^\dagger \hat{a}_j + \left( J_1 - \frac{\kappa}{2} \right) \hat{a}_j^\dagger \hat{b}_j \right] \\
& + \sum_{n=1}^N \sum_{\alpha \in \{a,b\}} \left[ -i \frac{\kappa}{2} \hat{\alpha}_n^\dagger \hat{\alpha}_n + g (\hat{\alpha}_n^\dagger \hat{\sigma}_n^- + \text{H.c.}) \right],
\end{aligned} \tag{1}$$

where  $\hat{\sigma}_n^- = (\hat{\sigma}_n^+)^\dagger = |g_n\rangle\langle e_n|$  is the pseudospin ladder operator of the  $n$ th atom,  $\Delta = \Delta_0 - i\gamma/2$  with frequency detuning  $\Delta_0$ ,  $\hat{a}_j$  and  $\hat{b}_j$  annihilate photons at sublattices  $a$  and  $b$  of the  $j$ th unit cell (see Fig. 1),  $g$  is the photon-emitter interacting strength, and  $j_n$  labels the unit cell at which the  $n$ th atom is located. Unless otherwise specified, we assume  $\gamma = \kappa$ .

*Chiral and Hidden Bound States.*—We couple a single emitter to the sublattice  $\alpha \in \{a, b\}$  within the unit cell  $j_0$  of the bath, and study the bound states lying within the regimes of both line and point gaps of the SSH bath. In the single-excitation subspace, the bound state using periodic boundary conditions (PBCs) can be written as  $|\psi_b\rangle = [L^{-1/2} \sum_k (c_{k,a} \hat{a}_k^\dagger + c_{k,b} \hat{b}_k^\dagger) + c_e \hat{\sigma}_{j_0}^+] |g\rangle \otimes |\text{vac}\rangle$ , with  $\hat{\alpha}_k = L^{-1/2} \sum_j e^{-ikj} \hat{\alpha}_j$  ( $\alpha = a, b$ ), which satisfies  $\hat{H}_{\text{eff}}(k) |\psi_b\rangle = E_b |\psi_b\rangle$ . For the photon-emitter bound states, we require  $c_e \neq 0$ . This yields [75]

$$\det [E_b - \Delta - \Sigma(E_b)] = 0, \tag{2}$$

where  $\Sigma(z)$  is the atomic self-energy, given by

$$\Sigma(z) = \frac{1}{L} \sum_k \mathbf{g}_k^\dagger (z - H_k)^{-1} \mathbf{g}_k, \tag{3}$$

with the bath's Bloch Hamiltonian  $H_k = -i\frac{\kappa}{2}\tau_0 + (J_1 + J_2 \cos k)\tau_x + (J_2 \sin k - i\kappa/2)\tau_y$ , and  $\mathbf{g}_k = [g_a e^{-ikj_0}, g_b e^{-ikj_0}]^T$  ( $g_a, g_b \in \{0, g\}$ ).

In the presence of line gap for  $|J_2| < |J_1 - \kappa/2|$ , we can analytically solve the real-space wavefunction of the bound state with  $E_b = -i\kappa/2$  for  $\Delta = -i\kappa/2$  [75]. For the emitter coupled to the sublattice  $a$ , we have  $c_{j,a} = 0$ ,  $c_{j,b} = -g c_e (-J_2)^{j-j_0} (J_1 - \kappa/2)^{-j+j_0-1}$  if  $j \geq j_0$ , and  $c_{j,b} = 0$  if  $j < j_0$ . For the emitter coupled to the sublattice  $b$ , we have  $c_{j,b} = 0$ ,  $c_{j,a} = g c_e J_2^{j_0-j} (-J_1 - \kappa/2)^{j-j_0-1}$  if  $j \leq j_0$ , and  $c_{j,a} = 0$  if  $j > j_0$ . These indicate that the bound state lying within the line gap [see red filled square marker in Fig. 2(a)] shows perfect chiral photon weight  $|c_j|^2$  for  $\Delta = -i\kappa/2$ , as shown in Fig. 2(b1). Such a chiral bound state can be interpreted as a boundary between two semi-infinite chains with different topology [12], its chirality thus depends on the sublattice  $a$  or  $b$  which the emitter is coupled to, and is insensitive to the NHSE. Note that the chirality of the bound state is sensitive to  $\Delta$  (see SM in Ref. [75]).

As a comparison, we calculate the bound state lying inside the point gap, which can be analytically solved out for  $J_1 = \kappa/2$  [75]. The self-energy of the bound state is obtained as

$$\Sigma(E_b) = \begin{cases} -\frac{g^2 (E_b + \frac{i\kappa}{2})}{J_2^2 - (E_b + \frac{i\kappa}{2})^2}, & |\kappa J_2| < |J_2^2 - (E_b + i\kappa/2)^2| \\ 0, & |\kappa J_2| > |J_2^2 - (E_b + i\kappa/2)^2| \end{cases} \tag{4}$$

The analytical results for the real-space wavefunctions are provided in SM [75]. The self-energy in Eq. (S36) vanishes for  $E_b$  lying inside the loop of the point gap, dubbed hidden bound state [72]. In contrast to conventional bound states, such a bound state exhibits skin-mode-like localization independent of  $\Delta$  [see Fig. 2(c,d1,d2) and also (b2)], which is determined by the NHSE associated with the point-gap topology of the bath. Note that the emergence of hidden bound states does not rely on the coupling strength  $g$  (see SM in Ref. [75]).

*Chiral-Extended Dressed States.*—In addition to localized chiral and hidden bound states, we identify an *unique in-gap photon-emitter dressed state*, exhibiting the chiral and extended mode distribution under OBCs. We consider the system parameter satisfying  $J_2 = J_1 \pm \kappa/2$ , where the line band-gap closes (with the appearance of an exceptional point) under PBCs [see the PBC spectrum in Fig. 3(a)]. According to the non-Bloch bulk-boundary correspondence in a generalized Brillouin zone [75], the true topological-phase transition point of band topology is determined by  $J_1 = \pm \sqrt{J_2^2 + (\kappa/2)^2}$ . It is

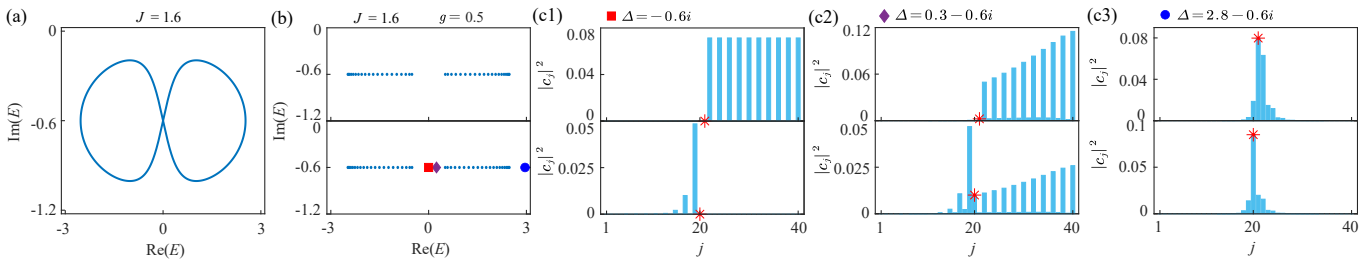


FIG. 3. Single-excitation spectrum of the SSH bath at transition point  $J_2 = J_1 - \kappa/2$  under (a) PBCs, and (b) OBCs (top plot). The markers, shown in bottom plot of (b), denote the eigenenergies of the dressed states of a single emitter coupled to the chain for different values of  $\Delta$ . The corresponding site-resolved photon weights  $|c_j|^2$  are shown in (c1-c3) under OBCs, where the emitter is coupled to the sublattice  $a$  (b), denoted by the red asterisk, for the top (bottom) plot. The parameters used are  $g = 0.5$ ,  $\kappa = 1.2$ ,  $J_1 = 1.6$ ,  $J_2 = 1.0$  and  $L = 20$ .

thus topologically trivial for  $J_2 = J_1 - \kappa/2$  with  $J_1\kappa \geq 0$  [see OBC spectrum in the top plot of Fig. 3(b)]. Unless otherwise specified, we consider this condition for system parameters below.

We first study a single emitter coupled to the sublattice  $\alpha \in \{a, b\}$  of the unit cell  $j_0$ . In the single-excitation subspace under OBC, the photon-emitter dressed state is written as  $|\psi_d\rangle = (\sum_{j,\alpha \in \{a,b\}} c_{j,\alpha} \hat{\alpha}_j^\dagger + c_e \hat{\sigma}^+) |g\rangle \otimes |0\rangle$ , which satisfies  $\hat{H}_{\text{eff}} |\psi_d\rangle = E_d |\psi_d\rangle$ . Then, we achieve

$$\Delta c_e + g c_{j_0, \alpha} = E_d c_e, \quad (5)$$

$$g c_e \delta_{j, j_0} \delta_{\alpha, a} + J_2 (c_{j, b} + c_{j-1, b}) = (E_d + i\kappa/2) c_{j, a}, \quad (6)$$

$$g c_e \delta_{j, j_0} \delta_{\alpha, b} + (J_2 + \kappa) c_{j, a} + J_2 c_{j+1, a} = (E_d + i\kappa/2) c_{j, b}. \quad (7)$$

For  $\Delta = -i\kappa/2$ , we can find the analytical solution for the dressed state with its eigenenergy  $E_d = \Delta$ . In this case, when the emitter is coupled to the sublattice  $a$  ( $\alpha = a$ ) in Eqs. (5-7), we obtain  $c_{j, a} = 0$ ,  $c_{j, b} = 0$  for  $j < j_0$ ,  $c_e = -J_2 c_{j, b} / g$  for  $j = j_0$ , and  $c_{j, b} = -c_{j-1, b}$  for  $j > j_0$ . The analytical results indicate that the in-gap photon-emitter dressed state exhibits an unconventional feature different from the one of the bound state when the emitter is coupled to the sublattice  $a$ . In addition to the chiral property with its eigenstate only distributed on the right side of the emitter, the dressed state is uniformly distributed along the  $b$  sites under OBC, as shown in the top plot of Fig. 3(c1) [Its eigenenergy is indicated by the red square marker in the bottom plot of Fig. 3(b)]. Noticeably, the chiral and extended photon-emitter dressed states are quite robust against the disordered-distributed cavity frequencies and disordered photonic hopping between cavities, as explained in SM [75]. Note that the extended photon profiles are influenced by the unequal decay rates  $\gamma$  and  $\kappa$  of the emitter and photon (see details in SM [75]).

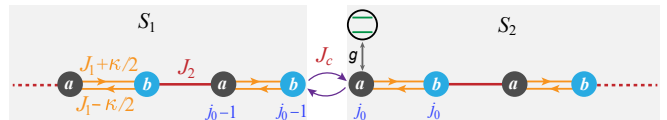


FIG. 4. Schematic for understanding the chiral and extended dressed state. when the emitter is coupled to the sublattice  $a$  under OBC, the hybrid system is divided into  $S_1$  and  $S_2$  subsystems by breaking the intercell coupling  $J_c = J_2$  that exists on the left side of the sublattice lattice  $a$  at the unit cell  $j_0$ .

In contrast, when the emitter is coupled to the sublattice  $b$  ( $\alpha = b$ ) in Eqs. (5-7), we obtain  $c_{j, b} = 0$ ,  $c_{j-1, a} = -J_2 c_{j, a} / (J_2 + \kappa)$  for  $j < j_0$ ,  $c_e = -(J_2 + \kappa) c_{j, a} / g$  for  $j = j_0$ , and  $c_{j, a} = 0$  for  $j > j_0$ . It turns out that the in-gap photon-emitter dressed state is bounded, and its photonic profile [see the bottom plot of Fig. 3(c1)] is localized at the left side of the emitter, i.e., showing the emergence of a chiral bound state.

The physical intuition of the appearance of the in-gap chiral and extended photon-emitter dressed states for  $\Delta = -i\kappa/2$  with  $J_2 = J_1 - \kappa/2$  can be attributed to the competition of topological-edge localization and non-Hermitian skin-mode localization with the combination of the non-Bloch bulk-boundary correspondence of a non-Hermitian topological bath. Namely, when the emitter is coupled to the sublattice  $a$  under OBC, we divide the photon-emitter system into two subsystems  $S_1$  and  $S_2$ , by breaking the intercell coupling  $J_c = J_2$  that exists on the left side of the sublattice lattice  $a$  at the unit cell  $j_0$ , as shown in Fig. 4. The subsystem  $S_1$  is topologically trivial, while the subsystem  $S_2$  hosts an in-gap topological edge mode where the emitter acts as the effective boundary of  $S_2$ . Instead of topological-edge localization on the left side of the subsystem  $S_2$ , the competition from the opposite mode localization towards the right side induced by NHSE leads to the extended mode distribution along the  $S_2$  at  $J_2 = J_1 - \kappa/2$  [76, 77]. The coupling of the trivial subsystem  $S_1$  to  $S_2$  only has a minor effect on the dressed state due to

its in-gap topological protection and zero occupations on  $a$  sublattices. Here, the broken bulk-boundary correspondence of the topological bath due to NHSE excludes the coupling of the photon-emitter dressed state with the edge states of the SSH bath. However, when the emitter is coupled to the sublattice  $b$ , two subsystems  $S_1$  and  $S_2$  are constructed by breaking the intercell coupling  $J_c = J_2$  that exists on the right side of the sublattice  $b$  at the unit cell  $(j_0 - 1)$ . In this case, both topological edge-mode localization and NHSE lead to the formation of the chiral localized in-gap bound state.

For arbitrary  $\Delta$ , we can still achieve the analytical solution of the eigenenergy  $E_d = E - i\kappa/2$  for the dressed state [75], with  $E$  satisfying

$$E - \Delta_0 - g^2 \sum_{m=1}^{2L} \frac{|\varphi_{m,\alpha}(j_0)|^2}{(E - \varepsilon_m)\mathcal{N}_m} = 0, \quad (8)$$

where  $\varepsilon_m = (-1)^m \sqrt{2\bar{J}_1 J_2 \cos \theta_m + \bar{J}_1^2 + J_2^2}$ , with  $\bar{J}_1 = \sqrt{(J_1 - \kappa/2)(J_1 + \kappa/2)}$ , and real number  $\theta_m$ , is the analytical eigenvalue of the non-Hermitian bath, and  $\varphi_{m,\alpha}(j)$  ( $\alpha = a, b$ ) is the element of the analytical eigenvectors of the Hermitian SSH lattice in the similarity-transformed basis with  $\mathcal{H}_\alpha = S_\alpha^{-1} \mathcal{H}_\alpha S_\alpha$  ( $\mathcal{H}_\alpha$  is the Hamiltonian matrix of  $\mathcal{H}_{\text{eff}}$  for the emitter coupled to the sublattice  $\alpha$ , and  $S_\alpha$  is the diagonal matrix  $\text{diag}[1, r^{-(j_0 - \delta_{\alpha,a})}, r^{1 - (j_0 - \delta_{\alpha,a})}, \dots, r^{L - (j_0 - \delta_{\alpha,a})}]$  with  $r = \sqrt{(J_1 + \kappa/2)/(J_1 - \kappa/2)}$ , see details in Ref. [75]), and  $\mathcal{N}_m$  is a normalization. This analytical result provides us an additional understanding of the chiral and extended dressed states for  $\alpha = a$ : in the similarity-transformed basis, the photon-emitter dressed state is bound with the photon weight power-law decaying towards the right side of the emitter [12]. After employing the inverse of the similarity transformation, the bound state becomes extended due to the power-law increase for each element of  $S_a$  starting at the site  $j_0$ . In addition, the analytical result of the photon weight  $|c_j|^2$  of the dressed state is shown in SM [75].

Figure 3(c2) shows the photon weight  $|c_j|^2$  with  $\Delta \neq -i\kappa/2$  for the emitter coupled to the sublattice  $\alpha = a$  ( $\alpha = b$ ) in the top (bottom) plot. The extended dressed states remain chiral with the uniform site-resolved photon weight for  $\alpha = a$ , while the bound state becomes extended distribution for  $\alpha = b$ . Note that there exist only bound states when the  $\Delta$  is set to be outside the middle gap of the OBC spectrum [see Fig. 3(c3)].

*Two Emitters.*—We now consider the consequences of such dressed states when two quantum emitters are coupled to the bath with  $J_2 = J_1 - \kappa/2$ . The bound states can mediate the emitter-emitter interactions, giving rise to the exotic many-body phases [12]. The distance of two interacting emitters is determined by the localization length of the bound state, leading to short-range interactions. In contrast, the extended in-gap dressed state can mediate long-range interactions,

and its chiral character causes the directional interactions between emitters.

In order to demonstrate such long-range interactions, we calculate the non-unitary real-time dynamics governed by  $|\psi_t\rangle = e^{-i\mathcal{H}_{\text{eff}}t} |\psi_0\rangle$  for two emitters (labeled as 1 and 2) coupled to sites  $j_{1,\alpha_1}$  and  $j_{2,\alpha_2}$  ( $\alpha_1, \alpha_2 = a$  or  $b$ ) of the bath with  $j_{2,\alpha_2} > j_{1,\alpha_1}$ , respectively. The initial state is chosen as one excited emitter  $|e_1\rangle$  or  $|e_2\rangle$  with  $|\psi_0\rangle = |e_n\rangle |\text{vac}\rangle$  ( $n = 1$  or  $2$ ), and the time-evolved state can be expanded as  $|\psi_t\rangle = \left( \sum_{m=1}^{2N} c_m(t) |\varphi_m^R\rangle \langle \text{vac}| + \sum_{n=1}^2 c_{e_n}(t) |e_n\rangle \langle g| \right) |gg\rangle \otimes |\text{vac}\rangle$  ( $|\varphi_m^R\rangle$  is the right eigenvector of the non-Hermitian bath [75]). Using the resolvent method [78, 79], we can express  $\mathbf{c}_e(t) = [c_{e_1}(t), c_{e_2}(t)]^T$  as [75]

$$\mathbf{c}_e(t) = \frac{i}{2\pi} \int_{-\infty}^{+\infty} dE \mathcal{G}_p(E + i0^+) e^{-iEt} \mathbf{c}_e(0), \quad (9)$$

where the Green's function  $\mathcal{G}_p(z)$  are given by

$$\mathcal{G}_p(E) = \begin{pmatrix} \frac{1}{E - \Delta - \mathcal{T}(\alpha_1, \alpha_1)} & \frac{1}{E - \mathcal{F}(\alpha_1, \alpha_2) \mathcal{T}(\alpha_1, \alpha_2)} \\ \frac{1}{E - \mathcal{F}(\alpha_2, \alpha_1) \mathcal{T}(\alpha_1, \alpha_2)} & \frac{1}{E - \Delta - \mathcal{T}(\alpha_2, \alpha_2)} \end{pmatrix}, \quad (10)$$

with

$$\mathcal{T}(\alpha_1, \alpha_2) = g^2 \sum_{m=1}^{2L} \frac{\varphi_{m,\alpha_1}(j_{1,\alpha_1}) \varphi_{m,\alpha_2}(j_{2,\alpha_2})}{(E - \varepsilon_m + i\kappa/2) \mathcal{N}_m}, \quad (11)$$

$$\mathcal{F}(\alpha_1, \alpha_2) = \frac{(J_1 + \kappa/2)^{\frac{j_{1,\alpha_1} - j_{2,\alpha_2} + \delta_{\alpha_1,b} - \delta_{\alpha_2,b}}{2}}}{(J_1 - \kappa/2)^{\frac{j_{1,\alpha_1} - j_{2,\alpha_2} + \delta_{\alpha_1,b} - \delta_{\alpha_1,b}}{2}}}. \quad (12)$$

According to Eqs. (9)-(12), the main contribution from the diagonal elements of the Green function  $\mathcal{G}_p(z)$  to the time evolution is the dressed state for small  $g$  and  $\Delta = -i\kappa/2$ . The off-diagonal elements contribute to the state exchanges between two emitters. Remarkably, such state exchange is asymmetrical [see Eq. (12)]. To be specific, when the emitter at the site  $j_{2,\alpha_2}$  is initially excited, there is no excitation transferred to the emitter at the site  $j_{1,\alpha_1}$  for the large distance  $|j_{1,\alpha_1} - j_{2,\alpha_2}|$  between them due to the power-law decay of  $\mathcal{F}(\alpha_1, \alpha_2)$ . Figure 5 the excited-state probability  $C_{e,i} = |c_{e_i}(t)|^2$  ( $i = 1, 2$ ) for two emitters coupled to sites  $j_{1,\alpha_1}$  and  $j_{2,\alpha_2}$  of the bath, where the emitter, coupled to the site  $j_{1,a}$ ,  $j_{2,a}$ ,  $j_{1,b}$ , and  $j_{2,b}$ , is initially excited for (a-d), respectively. When the first emitter coupled to the site  $j_{1,a}$  is initially in the excited state, this will excite the second emitter at the  $j_{2,\alpha}$ , even in a very large separation away from the first emitter [see Fig. 5(a,c)], which is limited by the intrinsic dissipation of the bath. In contrast, when the second emitter coupled to the site  $j_{2,\alpha}$  is initially in the excited state, no excitation is transferred to the first emitter at

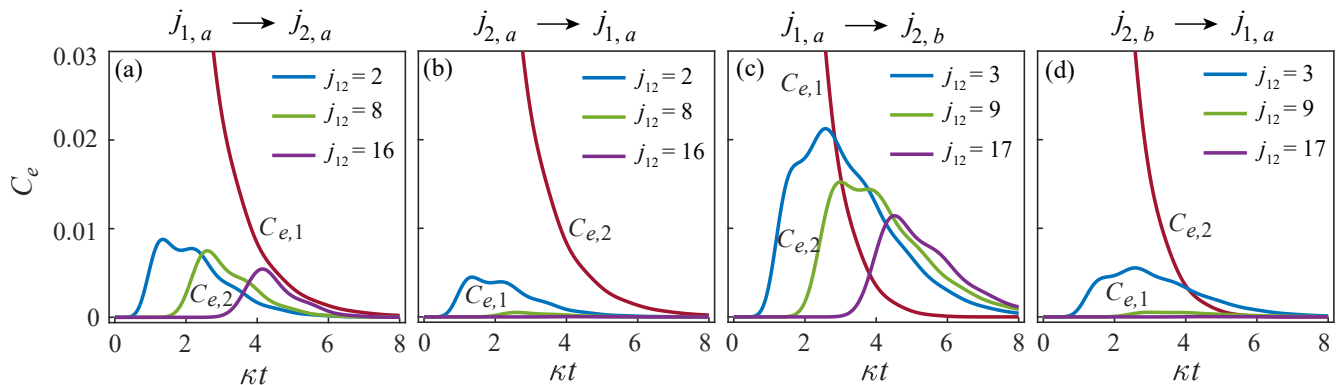


FIG. 5. Excited-state probability  $C_{e,i} = |c_{e_i}(t)|^2$  ( $i = 1, 2$ ) for two emitters coupled to sites  $j_{1,\alpha_1}$  and  $j_{2,\alpha_2}$  ( $\alpha_1, \alpha_2 = a$  or  $b$ , and  $j_{2,\alpha_2} > j_{1,\alpha_1}$ ) of the bath, where the emitter, coupled to the site  $j_{1,a}$ ,  $j_{2,a}$ ,  $j_{1,a}$ , and  $j_{2,b}$ , is initially excited for (a-d), respectively. The parameters used are  $g = 0.4$ ,  $\kappa = 0.4$ ,  $J_1 = 1.2$ ,  $J_2 = 1.0$ ,  $\Delta = -0.2i$ , and  $L = 100$ .

the site  $j_{1,a}$  for a slight separation between them. The nonreciprocal long-range emitter-emitter interaction can induce exotic many-body phenomena, which is worth further investigation.

*Conclusion and Outlook.*—In summary, we have studied the conventional chiral and hidden bound states lying inside the line and point gaps of the 1D non-Hermitian topological bath, to which a single emitter is coupled. Most remarkably, we found a unique photon-emitter dressed state without Hermitian counterparts, showing the chiral and extended distribution on just one side of the emitter along the bath. Such unconventional dressed states mediate the nonreciprocal long-range emitter-emitter interactions with the range limited by the bath dissipation. Our study opens many possible directions for future studies, e.g., the study of novel many-body phases of emergent spin models with long-range interactions of many emitters and peculiar extended dressed states in higher-dimensional non-Hermitian topological baths.

T.L. acknowledges the support from National Natural Science Foundation of China (Grant No. 12274142), the Fundamental Research Funds for the Central Universities (Grant No. 2023ZYGXZR020), Introduced Innovative Team Project of Guangdong Pearl River Talents Program (Grant No. 2021ZT09Z109), and the Startup Grant of South China University of Technology (Grant No. 20210012). X.W. is supported by the National Natural Science Foundation of China (NSFC; No. 12174303 and Grant No. 11804270), and the Fundamental Research Funds for the Central Universities (No. xzy012023053). F.N. is supported in part by: Nippon Telegraph and Telephone Corporation (NTT) Research, the Japan Science and Technology Agency (JST)[via the Quantum Leap Flagship Program (Q-LEAP), and the Moonshot R&D Grant Number JPMJMS2061], the Asian Office of Aerospace Research and Development (AOARD) (via Grant No. FA2386-20-

1-4069), and the Office of Naval Research (ONR) Global (via Grant No. N62909-23-1-2074).

\* These authors contributed equally

† E-mail: liutao0716@scut.edu.cn

- [1] A. González-Tudela and J. I. Cirac, “Quantum emitters in two-dimensional structured reservoirs in the nonperturbative regime,” *Phys. Rev. Lett.* **119**, 143602 (2017).
- [2] A. González-Tudela and J. I. Cirac, “Markovian and non-Markovian dynamics of quantum emitters coupled to two-dimensional structured reservoirs,” *Phys. Rev. A* **96**, 043811 (2017).
- [3] P. Bienias, I. Boettcher, R. Belyansky, A. J. Kollár, and A. V. Gorshkov, “Circuit quantum electrodynamics in hyperbolic space: From photon bound states to frustrated spin models,” *Phys. Rev. Lett.* **128**, 013601 (2022).
- [4] A. F. Kockum, G. Johansson, and F. Nori, “Decoherence-free interaction between giant atoms in waveguide quantum electrodynamics,” *Phys. Rev. Lett.* **120**, 140404 (2018).
- [5] I. García-Elcano, A. González-Tudela, and J. Bravo-Abad, “Tunable and robust long-range coherent interactions between quantum emitters mediated by Weyl bound states,” *Phys. Rev. Lett.* **125**, 163602 (2020).
- [6] X. Wang, T. Liu, A. F. Kockum, H.-R. Li, and F. Nori, “Tunable chiral bound states with giant atoms,” *Phys. Rev. Lett.* **126**, 043602 (2021).
- [7] L. Leonforte, A. Carollo, and F. Ciccarello, “Vacancy-like dressed states in topological waveguide qed,” *Phys. Rev. Lett.* **126**, 063601 (2021).
- [8] D. De Bernardis, Z.-P. Ciani, I. Carusotto, M. Hafezi, and P. Rabl, “Light-matter interactions in synthetic magnetic fields: Landau-photon polaritons,” *Phys. Rev. Lett.* **126**, 103603 (2021).
- [9] J. Perczel, J. Borregaard, D. E. Chang, H. Pichler, S. F. Yelin, P. Zoller, and M. D. Lukin, “Topological quantum optics in two-dimensional atomic arrays,” *Phys. Rev. Lett.* **119**, 023603 (2017).
- [10] R. J. Bettles, J. Minář, C. S. Adams, I. Lesanovsky,

- and B. Olmos, “Topological properties of a dense atomic lattice gas,” *Phys. Rev. A* **96**, 041603 (2017).
- [11] S. Barik, A. Karasahin, C. Flower, T. Cai, H. Miyake, W. DeGottardi, M. Hafezi, and E. Waks, “A topological quantum optics interface,” *Science* **359**, 666 (2018).
- [12] M. Bello, G. Platero, J. I. Cirac, and A. González-Tudela, “Unconventional quantum optics in topological waveguide QED,” *Sci. Adv.* **5**, eaaw0297 (2019).
- [13] E. Kim, X. Zhang, V. S. Ferreira, J. Banker, J. K. Iverson, A. Sipahigil, M. Bello, A. González-Tudela, M. Mirhosseini, and O. Painter, “Quantum electrodynamics in a topological waveguide,” *Phys. Rev. X* **11**, 011015 (2021).
- [14] C. Vega, M. Bello, D. Porras, and A. González-Tudela, “Qubit-photon bound states in topological waveguides with long-range hoppings,” *Phys. Rev. A* **104**, 053522 (2021).
- [15] C. Vega, D. Porras, and A. González-Tudela, “Topological multimode waveguide QED,” *Phys. Rev. Res.* **5**, 023031 (2023).
- [16] M. Bello, G. Platero, and A. González-Tudela, “Spin many-body phases in standard- and topological-waveguide QED simulators,” *PRX Quantum* **3**, 010336 (2022).
- [17] W. Nie, M. Antezza, Y.-x. Liu, and F. Nori, “Dissipative topological phase transition with strong system-environment coupling,” *Phys. Rev. Lett.* **127**, 250402 (2021).
- [18] D. E. Chang, J. S. Douglas, A. González-Tudela, C.-L. Hung, and H. J. Kimble, “Colloquium: Quantum matter built from nanoscopic lattices of atoms and photons,” *Rev. Mod. Phys.* **90**, 031002 (2018).
- [19] J.-S. Tang, W. Nie, L. Tang, M. Chen, X. Su, Y. Lu, F. Nori, and K. Xia, “Nonreciprocal single-photon band structure,” *Phys. Rev. Lett.* **128**, 203602 (2022).
- [20] A. S. Sheremet, M. I. Petrov, I. V. Iorsh, A. V. Poshakinskiy, and A. N. Poddubny, “Waveguide quantum electrodynamics: Collective radiance and photon-photon correlations,” *Rev. Mod. Phys.* **95**, 015002 (2023).
- [21] X. Wang, H.-B. Zhu, T. Liu, and F. Nori, “Realizing quantum optics in structured environments with giant atoms,” *Phys. Rev. Res.* **6**, 013279 (2024).
- [22] Z.-G. Lu, G. Tian, X.-Y. Lü, and C. Shang, “Topological quantum batteries,” arXiv:2405.03675 (2024).
- [23] A. González-Tudela, A. Reiserer, J. J. García-Ripoll, and F. J. García-Vidal, “Light-matter interactions in quantum nanophotonic devices,” *Nat. Rev. Phys.* **6**, 166 (2024).
- [24] Y. Ashida, Z. Gong, and M. Ueda, “Non-Hermitian physics,” *Adv. Phys.* **69**, 249 (2020).
- [25] T. Gao, E. Estrecho, K. Y. Bliokh, T. C. H. Liew, M. D. Fraser, S. Brodbeck, M. Kamp, C. Schneider, S. Höfling, Y. Yamamoto, F. Nori, Y. S. Kivshar, A. G. Truscott, R. G. Dall, and E. A. Ostrovskaya, “Observation of non-Hermitian degeneracies in a chaotic exciton-polariton billiard,” *Nature* **526**, 554 (2015).
- [26] F. Monifi, J. Zhang, Ş. K. Özdemir, B. Peng, Y.-x. Liu, F. Bo, F. Nori, and L. Yang, “Optomechanically induced stochastic resonance and chaos transfer between optical fields,” *Nat. Photon.* **10**, 399 (2016).
- [27] J. Zhang, B. Peng, Ş. K. Özdemir, K. Pichler, D. O. Krimer, G. Zhao, F. Nori, Y.-x. Liu, S. Rotter, and L. Yang, “A phonon laser operating at an exceptional point,” *Nat. Photon.* **12**, 479 (2018).
- [28] Tony E. Lee, “Anomalous edge state in a non-Hermitian lattice,” *Phys. Rev. Lett.* **116**, 133903 (2016).
- [29] D. Leykam, K. Y. Bliokh, C. Huang, Y. D. Chong, and F. Nori, “Edge modes, degeneracies, and topological numbers in non-Hermitian systems,” *Phys. Rev. Lett.* **118**, 040401 (2017).
- [30] Y. Xu, S. T. Wang, and L. M. Duan, “Weyl exceptional rings in a three-dimensional dissipative cold atomic gas,” *Phys. Rev. Lett.* **118**, 045701 (2017).
- [31] Z. Gong, Y. Ashida, K. Kawabata, K. Takasan, S. Higashikawa, and M. Ueda, “Topological phases of non-Hermitian systems,” *Phys. Rev. X* **8**, 031079 (2018).
- [32] B. Peng, S. K. Özdemir, S. Rotter, H. Yilmaz, M. Liertzer, F. Monifi, C. M. Bender, F. Nori, and L. Yang, “Loss-induced suppression and revival of lasing,” *Science* **346**, 328 (2014).
- [33] R. El-Ganainy, K. G. Makris, M. Khajavikhan, Z. H. Musslimani, S. Rotter, and D. N. Christodoulides, “Non-Hermitian physics and PT symmetry,” *Nat. Phys.* **14**, 11 (2018).
- [34] S. Yao and Z. Wang, “Edge states and topological invariants of non-Hermitian systems,” *Phys. Rev. Lett.* **121**, 086803 (2018).
- [35] K. Zhang, Z. Yang, and C. Fang, “Correspondence between winding numbers and skin modes in non-Hermitian systems,” *Phys. Rev. Lett.* **125**, 126402 (2020).
- [36] K. Yokomizo and S. Murakami, “Non-Bloch band theory of non-Hermitian systems,” *Phys. Rev. Lett.* **123**, 066404 (2019).
- [37] S. Yao, F. Song, and Z. Wang, “Non-Hermitian Chern bands,” *Phys. Rev. Lett.* **121**, 136802 (2018).
- [38] F. K. Kunst, E. Edvardsson, J. C. Budich, and E. J. Bergholtz, “Biorthogonal bulk-boundary correspondence in non-Hermitian systems,” *Phys. Rev. Lett.* **121**, 026808 (2018).
- [39] T. Liu, Y.-R. Zhang, Q. Ai, Z. Gong, K. Kawabata, M. Ueda, and F. Nori, “Second-order topological phases in non-Hermitian systems,” *Phys. Rev. Lett.* **122**, 076801 (2019).
- [40] F. Song, S. Yao, and Z. Wang, “Non-Hermitian skin effect and chiral damping in open quantum systems,” *Phys. Rev. Lett.* **123**, 170401 (2019).
- [41] J. Y. Lee, J. Ahn, H. Zhou, and A. Vishwanath, “Topological correspondence between Hermitian and non-Hermitian systems: Anomalous dynamics,” *Phys. Rev. Lett.* **123**, 206404 (2019).
- [42] K. Kawabata, T. Bessho, and M. Sato, “Classification of exceptional points and non-Hermitian topological semimetals,” *Phys. Rev. Lett.* **123**, 066405 (2019).
- [43] W. Nie, T. Shi, Y.-x. Liu, and F. Nori, “Non-Hermitian waveguide cavity QED with tunable atomic mirrors,” *Phys. Rev. Lett.* **131**, 103602 (2023).
- [44] Z. Y. Ge, Y. R. Zhang, T. Liu, S. W. Li, H. Fan, and F. Nori, “Topological band theory for non-Hermitian systems from the Dirac equation,” *Phys. Rev. B* **100**, 054105 (2019).
- [45] H. Zhou and J. Y. Lee, “Periodic table for topological bands with non-Hermitian symmetries,” *Phys. Rev. B* **99**, 235112 (2019).
- [46] H. Zhao, X. Qiao, T. Wu, B. Midya, S. Longhi, and

- L. Feng, “Non-Hermitian topological light steering,” *Science* **365**, 1163 (2019).
- [47] K. Kawabata, K. Shiozaki, M. Ueda, and M. Sato, “Symmetry and topology in non-Hermitian physics,” *Phys. Rev. X* **9**, 041015 (2019).
- [48] D. S. Borgnia, A. J. Kruchkov, and R.-J. Slager, “Non-Hermitian boundary modes and topology,” *Phys. Rev. Lett.* **124**, 056802 (2020).
- [49] T. Liu, J. J. He, T. Yoshida, Z.-L. Xiang, and F. Nori, “Non-Hermitian topological Mott insulators in one-dimensional fermionic superlattices,” *Phys. Rev. B* **102**, 235151 (2020).
- [50] K. Y. Bliokh, D. Leykam, M. Lein, and F. Nori, “Topological non-Hermitian origin of surface Maxwell waves,” *Nat. Comm.* **10**, 580 (2019).
- [51] K. Yokomizo and S. Murakami, “Scaling rule for the critical non-Hermitian skin effect,” *Phys. Rev. B* **104**, 165117 (2021).
- [52] N. Okuma, K. Kawabata, K. Shiozaki, and M. Sato, “Topological origin of non-Hermitian skin effects,” *Phys. Rev. Lett.* **124**, 086801 (2020).
- [53] Y. Yi and Z. Yang, “Non-Hermitian skin modes induced by on-site dissipations and chiral tunneling effect,” *Phys. Rev. Lett.* **125**, 186802 (2020).
- [54] T. Liu, J. J. He, Z. Yang, and F. Nori, “Higher-order Weyl-exceptional-ring semimetals,” *Phys. Rev. Lett.* **127**, 196801 (2021).
- [55] E. J. Bergholtz, J. C. Budich, and F. K. Kunst, “Exceptional topology of non-Hermitian systems,” *Rev. Mod. Phys.* **93**, 015005 (2021).
- [56] Y. Li, C. Liang, C. Wang, C. Lu, and Y.-C. Liu, “Gain-loss-induced hybrid skin-topological effect,” *Phys. Rev. Lett.* **128**, 223903 (2022).
- [57] C. Leefmans, A. Dutt, J. Williams, L. Yuan, M. Parto, F. Nori, S. Fan, and A. Marandi, “Topological dissipation in a time-multiplexed photonic resonator network,” *Nat. Phys.* **18**, 442 (2022).
- [58] K. Zhang, Z. Yang, and C. Fang, “Universal non-Hermitian skin effect in two and higher dimensions,” *Nat. Commun.* **13**, 2496 (2022).
- [59] M. Parto, C. Leefmans, J. Williams, F. Nori, and A. Marandi, “Non-Abelian effects in dissipative photonic topological lattices,” *Nat. Comm.* **14**, 1440 (2023).
- [60] Z. Ren, D. Liu, E. Zhao, C. He, K. K. Pak, J. Li, and G.-B. Jo, “Chiral control of quantum states in non-Hermitian spin-orbit-coupled fermions,” *Nat. Phys.* **18**, 385 (2022).
- [61] K. Kawabata, T. Numasawa, and S. Ryu, “Entanglement phase transition induced by the non-Hermitian skin effect,” *Phys. Rev. X* **13**, 021007 (2023).
- [62] K. Zhang, C. Fang, and Z. Yang, “Dynamical degeneracy splitting and directional invisibility in non-Hermitian systems,” *Phys. Rev. Lett.* **131**, 036402 (2023).
- [63] C.-A. Li, B. Trauzettel, T. Neupert, and S.-B. Zhang, “Enhancement of second-order non-Hermitian skin effect by magnetic fields,” *Phys. Rev. Lett.* **131**, 116601 (2023).
- [64] J. Liu, Z.-F. Cai, T. Liu, and Z. Yang, “Reentrant non-Hermitian skin effect in coupled non-Hermitian and Hermitian chains with correlated disorder,” *arXiv:2311.03777* (2023).
- [65] Z.-F. Cai, T. Liu, and Z. Yang, “Non-Hermitian skin effect in periodically driven dissipative ultracold atoms,” *Phys. Rev. A* **109**, 063329 (2024).
- [66] X. Li, J. Liu, and T. Liu, “Localization-delocalization transitions in non-Hermitian Aharonov-Bohm cages,” *Front. Phys.* **19**, 33211 (2024).
- [67] H.-Y. Wang, F. Song, and Z. Wang, “Amoeba formulation of non-Bloch band theory in arbitrary dimensions,” *Phys. Rev. X* **14**, 021011 (2024).
- [68] Y.-M. Hu, H.-Y. Wang, Z. Wang, and F. Song, “Geometric origin of non-Bloch  $\mathcal{PT}$  symmetry breaking,” *Phys. Rev. Lett.* **132**, 050402 (2024).
- [69] C. R. Leefmans, M. Parto, J. Williams, G. H. Y. Li, A. Dutt, F. Nori, and A. Marandi, “Topological temporally mode-locked laser,” *Nat. Phys.* **20**, 852 (2024).
- [70] F. Roccati, S. Lorenzo, G. Calajò, G. M. Palma, A. Carollo, and F. Ciccarello, “Exotic interactions mediated by a non-Hermitian photonic bath,” *Optica* **9**, 565 (2022).
- [71] Z. Gong, M. Bello, D. Malz, and F. K. Kunst, “Bound states and photon emission in non-Hermitian nanophotonics,” *Phys. Rev. A* **106**, 053517 (2022).
- [72] Z. Gong, M. Bello, D. Malz, and F. K. Kunst, “Anomalous behaviors of quantum emitters in non-Hermitian baths,” *Phys. Rev. Lett.* **129**, 223601 (2022).
- [73] L. Du, L. Guo, Y. Zhang, and A. F. Kockum, “Giant emitters in a structured bath with non-Hermitian skin effect,” *Phys. Rev. Res.* **5**, L042040 (2023).
- [74] F. Roccati, M. Bello, Z. Gong, M. Ueda, F. Ciccarello, A. Chenu, and A. Carollo, “Hermitian and non-Hermitian topology from photon-mediated interactions,” *Nat. Commun.* **15**, 2400 (2024).
- [75] See Supplemental Material for detailed derivations.
- [76] W. Zhu, W. X. Teo, L. Li, and J. Gong, “Delocalization of topological edge states,” *Phys. Rev. B* **103**, 195414 (2021).
- [77] W. Wang, X. Wang, and G. Ma, “Non-Hermitian morphing of topological modes,” *Nature* **608**, 50 (2022).
- [78] C. Cohen-Tannoudji, J. Dupont-Roc, and G. Grynberg, *Atom-Photon Interactions: Basic Process and Applications* (John Wiley and Sons, 1998).
- [79] E. N. Economou, *Green’s Functions in Quantum Physics* (Springer Berlin Heidelberg, 2006).

**SUPPLEMENTAL MATERIAL FOR “CHIRAL-EXTENDED PHOTON-EMITTER DRESSED STATES IN NON-HERMITIAN TOPOLOGICAL BATHS”**

**I. Effective non-Hermitian bath in single-excitation subspace**

As shown in the main text, we consider a set of  $N$  identical atoms, as quantum emitters, coupled to a 1D Su-Schrieffer–Heeger (SSH) photonic chain with  $L$  unit cells. The photonic chain consists of coupled cavities subjected to engineered nonlocal dissipation, as shown in Fig. 1 in the main text. Each two-level atom, with ground state  $|g\rangle$  and excited state  $|e\rangle$ , is coupled to each cavity in the lattice. Under the Markovian and rotating-wave approximations, the dissipative dynamics of the system (in the rotating frame) is governed by the Lindblad master equation [S1–S4]:

$$\frac{d\hat{\rho}}{dt} = -i \left[ \hat{\mathcal{H}}_e + \hat{\mathcal{H}}_p + \hat{\mathcal{H}}_{\text{int}}, \hat{\rho} \right] + \gamma \sum_{n=1}^N \mathcal{D}[\hat{\sigma}_n^-] \hat{\rho} + \kappa \sum_j \mathcal{D}[\hat{L}_j] \hat{\rho}, \quad (\text{S1})$$

where the Hamiltonians of atoms  $\hat{\mathcal{H}}_e$ , photonic SSH bath  $\hat{\mathcal{H}}_p$  and photon-emitter interaction  $\hat{\mathcal{H}}_{\text{int}}$  are written as

$$\hat{\mathcal{H}}_e = \sum_{n=1}^N \Delta_0 \hat{\sigma}_n^+ \hat{\sigma}_n^-, \quad (\text{S2})$$

$$\hat{\mathcal{H}}_p = \sum_{j=1}^L \left( J_1 \hat{b}_j^\dagger \hat{a}_j + J_2 \hat{a}_{j+1}^\dagger \hat{b}_j + \text{H.c.} \right), \quad (\text{S3})$$

$$\hat{\mathcal{H}}_{\text{int}} = \sum_{n=1}^N \sum_{\alpha \in \{a,b\}} g \left( \hat{a}_{j_n}^\dagger \hat{\sigma}_n^- + \text{H.c.} \right). \quad (\text{S4})$$

Here,  $\hat{\sigma}_n^- = (\hat{\sigma}_n^+)^{\dagger} = |g_n\rangle\langle e_n|$  is the pseudospin ladder operator of the  $n$ th atom,  $\Delta_0$  is frequency detuning of the atom with respect to the cavity frequency,  $\hat{a}_j$  and  $\hat{b}_j$  annihilate photons at sublattices  $a$  and  $b$  of the  $j$ th unit cell (see Fig. 1 in the main text),  $g$  is the photon-emitter interacting strength, and  $j_n$  labels the unit cell at which the  $n$ th atom is located. Moreover,  $\hat{\rho}$  is the system density matrix, the Lindblad superoperator  $\mathcal{D}[\hat{\mathcal{L}}]\hat{\rho} = \hat{\mathcal{L}}\hat{\rho}\hat{\mathcal{L}}^\dagger - \{\hat{\mathcal{L}}^\dagger\hat{\mathcal{L}}, \hat{\rho}\}/2$  represents atomic and photonic dissipation,  $\gamma$  is the atomic decay rate, and  $\kappa$  denotes the photonic loss. In this work, we consider the nonlocal photon decay between two sublattices  $a$  and  $b$  in each unit cell with  $\hat{L}_j = \hat{a}_j - i\hat{b}_j$ .

We consider the single-excitation subspace with an initial state  $|\psi_0\rangle = \hat{\sigma}_n^+ |g\rangle \otimes |\text{vac}\rangle$ , here  $|g\rangle \equiv |g_1 g_2 \dots g_N\rangle$  and  $|\text{vac}\rangle$  is the photon vacuum state, and so as the initial density matrix  $\hat{\rho}_0 = |\psi_0\rangle\langle\psi_0|$ . Then, the master equation in Eq. (S1) can be solved as [S5–S8]

$$\hat{\rho}_t = e^{-i\hat{\mathcal{H}}_{\text{eff}}t} \hat{\rho}_0 e^{i\hat{\mathcal{H}}_{\text{eff}}^\dagger t} + p_t |g\rangle\langle g| \otimes |\text{vac}\rangle\langle\text{vac}|, \quad (\text{S5})$$

with

$$p_t = 1 - \text{Tr}[e^{-i\hat{\mathcal{H}}_{\text{eff}}t} \hat{\rho}_0 e^{i\hat{\mathcal{H}}_{\text{eff}}^\dagger t}]. \quad (\text{S6})$$

Therefore, when focusing only on the single-excitation subspace, the system’s dynamics is governed by the effective non-Hermitian Hamiltonian

$$\hat{\mathcal{H}}_{\text{eff}} = \hat{\mathcal{H}}_e + \hat{\mathcal{H}}_p + \hat{\mathcal{H}}_{\text{int}} - i\gamma/2 \sum_n \hat{\sigma}_n^+ \hat{\sigma}_n^- - i\kappa/2 \sum_j \hat{L}_j^\dagger \hat{L}_j. \quad (\text{S7})$$

Under periodic boundary conditions (PBCs), and using  $\hat{\alpha}_k = L^{-1/2} \sum_j e^{-ikj} \hat{\alpha}_j$  ( $\alpha = a, b$ ), the momentum-space Hamiltonian becomes

$$\hat{\mathcal{H}}_{\text{eff}}(k) = \Delta \sum_{n=1}^N \hat{\sigma}_n^+ \hat{\sigma}_n^- + \sum_k \hat{\mathbf{a}}_k^\dagger H_k \hat{\mathbf{a}}_k + \frac{1}{\sqrt{L}} \sum_{n=1}^N \sum_k \left( \hat{\sigma}_n^- \hat{\mathbf{a}}_k^\dagger \mathbf{g}_{kn} + \text{H.c.} \right), \quad (\text{S8})$$

where  $\Delta = \Delta_0 - i\gamma/2$ ,  $\hat{\mathbf{a}}_k \equiv [\hat{a}_k, \hat{b}_k]^T$ ,  $\mathbf{g}_{kn} = [g_a e^{-ikj_n}, g_b e^{-ikj_n}]^T$  with  $g_a, g_b \in \{0, g\}$ , and the Bloch Hamiltonian of the non-Hermitian SSH bath  $H_p(k)$  is

$$H_k = -i\frac{\kappa}{2}\tau_0 + (J_1 + J_2 \cos k)\tau_x + (J_2 \sin k - i\kappa/2)\tau_y, \quad (\text{S9})$$

with Pauli matrices  $\tau_i$  ( $i = x, y, z$ ) and identity matrix  $\tau_0$ .



## II. Bulk-boundary correspondence of a non-Hermitian SSH bath

As shown in Eq. (S9), the Bloch Hamiltonian of the non-Hermitian SSH bath is rewritten as

$$H_k = \mathcal{H}_k - i(\kappa/2)\tau_0, \quad \text{with } \mathcal{H}_k = (J_1 + J_2 \cos k) \tau_x + (J_2 \sin k - i\kappa/2) \tau_y, \quad (\text{S10})$$

where the Hamiltonians  $H_k$  and  $\mathcal{H}_k$  are topologically equivalent. The non-Hermitian skin effect leads to the breakdown of the conventional bulk-boundary correspondence. The topological-phase boundary can be recovered by the non-Bloch theory [S9], where the non-Bloch Hamiltonian for  $\mathcal{H}_k$  reads

$$\mathcal{H}_\beta = \begin{pmatrix} 0 & J_1 - \frac{\kappa}{2} + J_2\beta^{-1} \\ J_1 + \frac{\kappa}{2} + J_2\beta & 0 \end{pmatrix}. \quad (\text{S11})$$

One can obtain the eigenvalue equation for  $\beta$  as  $\det[\mathcal{H}_\beta - E] = 0$ . Therefore, we have

$$\left[ \left( J_1 - \frac{\kappa}{2} \right) + J_2\beta^{-1} \right] \left[ \left( J_1 + \frac{\kappa}{2} \right) + J_2\beta \right] = E^2. \quad (\text{S12})$$

This leads to two solutions

$$\beta_{1,2}(E) = \frac{[E^2 + \kappa^2/4 - J_1^2 - J_2^2] \pm \sqrt{[E^2 + \kappa^2/4 - J_1^2 - J_2^2]^2 - 4J_2^2(J_1^2 - \kappa^2/4)}}{2J_2(J_1 - \kappa/2)}, \quad (\text{S13})$$

where  $+$ ( $-$ ) corresponds to  $\beta_1$  ( $\beta_2$ ). Then, we obtain

$$\beta_1\beta_2 = \frac{J_1 + \kappa/2}{J_1 - \kappa/2}. \quad (\text{S14})$$

According to the generalized Bloch band theory [S10], we require  $|\beta_1| = |\beta_2|$ . This leads to

$$|\beta_1| = |\beta_2| = \sqrt{\left| \frac{J_1 + \kappa/2}{J_1 - \kappa/2} \right|}. \quad (\text{S15})$$

Due to chiral symmetry, we can obtain a generalized  $Q$  matrix [S9], defined as

$$Q(\beta) = |\tilde{\psi}_R(\beta)\rangle\langle\tilde{\psi}_L(\beta)| - |\psi_R(\beta)\rangle\langle\psi_L(\beta)| = \begin{pmatrix} 0 & q \\ q^{-1} & 0 \end{pmatrix}, \quad (\text{S16})$$

where  $|\tilde{\psi}_R(\beta)\rangle = \sigma_z|\psi_R(\beta)\rangle$  and  $|\tilde{\psi}_L(\beta)\rangle = \sigma_z|\psi_L(\beta)\rangle$ , with the right and left eigenvectors given by the following eigenequations

$$\mathcal{H}_\beta|\psi_R(\beta)\rangle = E(\beta)|\psi_R(\beta)\rangle, \quad \mathcal{H}_\beta^\dagger|\psi_L(\beta)\rangle = E^*(\beta)|\psi_L(\beta)\rangle. \quad (\text{S17})$$

The non-Bloch winding number  $\mathcal{W}$  is given by

$$\mathcal{W} = \frac{i}{2\pi} \int_{\text{GBZ}} \frac{dq}{q}, \quad (\text{S18})$$

where GBZ denotes the generalized Brillouin zone.

According to Eqs. (S16-S18), the true topological-phase transition points in the presence of non-Hermitian skin effects are given by

$$J_1 = \pm \sqrt{J_2^2 + \kappa^2/4}, \quad (\text{S19})$$

where the SSH bath is topologically nontrivial when  $J_1 \in (-\sqrt{J_2^2 + \kappa^2/4}, \sqrt{J_2^2 + \kappa^2/4})$ .

### III. Chiral and hidden bound states

Due to the particle number conservation of the system Hamiltonian  $\hat{\mathcal{H}}_{\text{eff}}(k)$  in Eq. (S8), in the single-excitation subspace, the bound state can be written as

$$|\psi_b\rangle = \left( \frac{1}{\sqrt{L}} \sum_k \mathbf{c}_k \hat{\mathbf{a}}_k^\dagger + \sum_{n=1}^N c_{e,n} \hat{\sigma}_n^+ \right) |g\rangle \otimes |\text{vac}\rangle, \quad (\text{S20})$$

with  $\mathbf{c}_k \equiv [c_{k,a}, c_{k,b}]^T$ , which satisfies  $\hat{\mathcal{H}}_{\text{eff}}(k) |\psi_b\rangle = E_b |\psi_b\rangle$ . Then, we obtain

$$\Delta \mathbf{c}_e + \frac{1}{L} \sum_k \mathbf{g}_k^\dagger \mathbf{c}_k = E_b \mathbf{c}_e, \quad \text{and} \quad H_k \mathbf{c}_k + \mathbf{g}_k \mathbf{c}_e = E_b \mathbf{c}_k, \quad (\text{S21})$$

for  $\forall k$ , where  $\mathbf{c}_e \equiv [c_{e,1}, c_{e,2}, \dots, c_{e,N}]^T$ , and  $\mathbf{g}_k \equiv [\mathbf{g}_{k1}, \mathbf{g}_{k2}, \dots, \mathbf{g}_{kN}]$ .

According to Eqs. (S21), we have

$$[E_b - \Delta - \Sigma(E_b)] \mathbf{c}_e = 0, \quad (\text{S22})$$

and for photon-emitter bound states, we require  $\mathbf{c}_e \neq 0$ . This yields

$$\det[E_b - \Delta - \Sigma(E_b)] = 0, \quad (\text{S23})$$

where  $\Sigma(z)$  is the self-energy of the emitters, given by

$$\Sigma(z) = \frac{1}{L} \sum_k \mathbf{g}_k^\dagger (z - H_k)^{-1} \mathbf{g}_k. \quad (\text{S24})$$

We then can determine the atomic and photonic weights as

$$|\mathbf{c}_e|^2 = \frac{1}{1 + \frac{1}{L} \sum_k \mathbf{g}_k^\dagger [(E_b - H_k)(E_b^* - H_k^\dagger)]^{-1} \mathbf{g}_k}, \quad \text{and} \quad \mathbf{c}_k = \frac{\mathbf{g}_k \mathbf{c}_e}{E_b - H_k}. \quad (\text{S25})$$

In this section, we are interest in a single emitter coupled to the sublattice  $a$  or  $b$  within the unit cell  $j_0$  of the bath, and study the bound states with its eigenenergy lying within the regimes of both line and point gaps of the non-Hermitian SSH bath. In this work, unless otherwise specified, we assume  $\gamma = \kappa$ .

#### A. Line gap and chiral bound state

In the presence of the line gap for the bath Hamiltonian  $H_k$ , to have a simple form of the analytical solution for the bound-state wavefunction in Eq. (S25), we solve the bound state for  $E_b = -i\kappa/2$ .

According to Eqs. (S23) and (S24), for  $E_b = -i\kappa/2$ , we immediately have

$$\Sigma(E_b) = 0, \quad \text{and} \quad \Delta = -i\kappa/2. \quad (\text{S26})$$

Then, according to Eq. (S25), the atomic weight  $|\mathbf{c}_e|^2$  for the emitter coupled to the sublattice  $a$  or  $b$  is, respectively, derived as

$$|c_{e,a}|^2 = \frac{1}{1 + \frac{g^2}{L} \sum_k |J_1 + J_2 e^{-ik} - \kappa/2|^{-2}}, \quad (\text{S27})$$

or

$$|c_{e,b}|^2 = \frac{1}{1 + \frac{g^2}{L} \sum_k |J_1 + J_2 e^{ik} + \kappa/2|^{-2}}. \quad (\text{S28})$$

(i) When the emitter is coupled to the sublattice  $a$ , the photonic weight  $c_{\alpha,k}$  ( $\alpha = a, b$ ) for  $\Delta = -i\kappa/2$  in momentum space is obtained as

$$c_{k,a} = 0, \quad \text{and} \quad c_{k,b} = -\frac{g_k c_{e,a}}{J_1 + J_2 e^{-ik} - \kappa/2}, \quad (\text{S29})$$

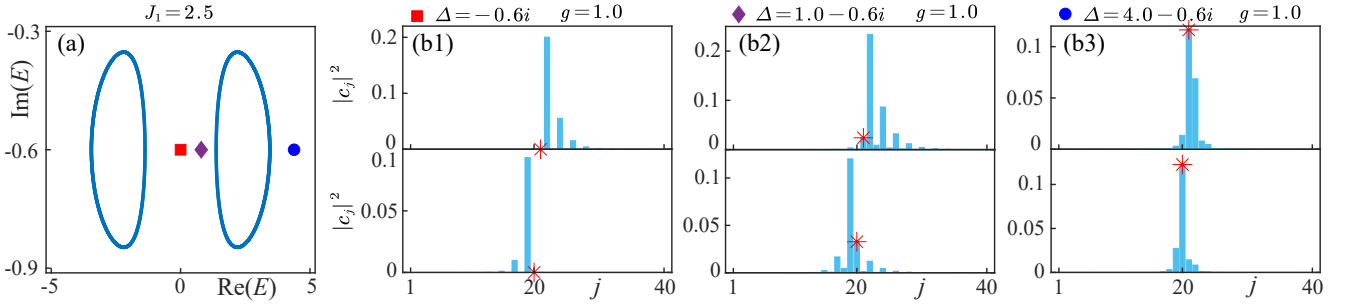


FIG. S1. Single-excitation line-gap spectrum (blue loops) of the bath  $H_k$  under PBCs for  $J_1 = 2.5$ . The markers denote the eigenenergies of the bound states of a single emitter coupled to the bath for different  $\Delta$ . The corresponding site-resolved photon weights  $|c_j|^2$  are shown in (b1-b3), where the emitter is coupled to the sublattice  $a$  ( $b$ ), denoted by the red asterisk, for the top (bottom) plot. The other parameters used are  $\kappa = 1.2$  and  $J_2 = 1.0$ .

where  $g_k = g e^{-ikj_0}$ . The real-space photonic profile can be obtained by the inverse Fourier transformation of Eq. (S29). This leads to  $c_{j,a} = 0$ , and

$$c_{j,b} = -\frac{g c_{e,a}}{L} \sum_k \frac{e^{ik(j-j_0)}}{J_1 + J_2 e^{-ik} - \frac{\kappa}{2}} = -\frac{g c_{e,a}}{2\pi i} \oint_{|y|=1} dy \frac{y^{j-j_0}}{J_2 + (J_1 - \kappa/2)y}. \quad (\text{S30})$$

According to Eq. (S30), for  $|J_2| < |J_1 - \kappa/2|$ , where the PBC spectrum of the SSH bath Hamiltonian  $H_k$  exhibits a linear gap, we obtain

$$c_{j,b} = \begin{cases} -\frac{g c_{e,a}}{J_1 - \kappa/2} \left(-\frac{J_2}{J_1 - \kappa/2}\right)^{j-j_0}, & j \geq j_0, \\ 0, & j < j_0. \end{cases} \quad (\text{S31})$$

(ii) When the emitter is coupled to the sublattice  $b$ , the photonic weight  $c_{\alpha,k}$  ( $\alpha = a, b$ ) for  $\Delta = -i\kappa/2$  in momentum space is obtained as

$$c_{k,a} = -\frac{g_k c_{e,b}}{J_1 + J_2 e^{ik} + \kappa/2}, \quad \text{and} \quad c_{k,b} = 0. \quad (\text{S32})$$

The real-space photonic profile is obtained by the inverse Fourier transformation of Eq. (S32). This leads to  $c_{j,b} = 0$ , and

$$c_{j,a} = -\frac{g c_{e,b}}{L} \sum_k \frac{e^{ik(j-j_0)}}{J_1 + J_2 e^{ik} + \frac{\kappa}{2}} = -\frac{g c_{e,b}}{2\pi i} \oint_{|y|=1} dy \frac{y^{j-j_0-1}}{J_2 y + J_1 + \kappa/2}. \quad (\text{S33})$$

According to Eq. (S33), for  $|J_2| < |J_1 + \kappa/2|$ , where the PBC spectrum exhibits a linear gap of the SSH bath Hamiltonian  $H_k$ , we obtain

$$c_{j,a} = \begin{cases} 0, & j > j_0, \\ \frac{g c_{e,b}}{J_2} \left(-\frac{J_1 + \kappa/2}{J_2}\right)^{j-j_0-1}, & j \leq j_0. \end{cases} \quad (\text{S34})$$

The above analytical results show that the bound state, with its eigenenergy lying inside the line gap, has its eigenstate located on just the left or right side of the emitter, depending on the sublattice  $a$  or  $b$  to which the emitter is coupled, for  $\Delta = -i\kappa/2$ , as shown in Fig. S1(a,b1). As explained in the main text, such a chiral bound state has a topological origin, which can be interpreted as the effective domain-wall state between two semi-infinite chains with different topology.

In spite of the nonreciprocal hopping, the bound state inside the line gap behaves more like conventional Hermitian bound states for  $\Delta = -i\kappa/2$  [S11]. When the detuning  $\Delta$  is deviated from the  $-i\kappa/2$ , the chirality of the bound states inside the line gap decreases due to coupling with the bulk bands of the bath, as shown in Fig. S1(b2). Outside the eigenenergy-spectrum range (i.e., above or below the two bands), the bound states do not exhibit chirality due to the absence of topological protection [see Fig. S1(b3)].

## B. Point gap and hidden bound state

We now consider the bound state with its eigenenergy enclosed by the point gap of the bath Hamiltonian  $H_k$ . To have a simple form of the analytical solution for the bound-state wavefunction in Eq. (S25), we solve the bound state for  $J_1 = \kappa/2$ . In this case, the eigenenergy of the bath Hamiltonian  $H_k$  in Eq. (S9) reads

$$E_0 = -i(\kappa/2) \pm [J_2(J_2 + \kappa e^{-ik})]^{-1/2}. \quad (\text{S35})$$

According to Eq. (3), the self energy of the bound state is written as

$$\Sigma(E_b) = \frac{g^2}{2\pi i} \oint_{|y|=1} dy \frac{E_b + \frac{i\kappa}{2}}{[(E_b + i\kappa/2)^2 - J_2^2] y - J_2 \kappa} = \begin{cases} -\frac{g^2(E_b + \frac{i\kappa}{2})}{J_2^2 - (E_b + \frac{i\kappa}{2})^2}, & |\kappa J_2| < |J_2^2 - (E_b + i\kappa/2)^2|, \\ 0, & |\kappa J_2| > |J_2^2 - (E_b + i\kappa/2)^2|. \end{cases} \quad (\text{S36})$$

It turns out that the self-energy vanishes when the  $E_b$  lies inside the loop of the point-gap spectrum. We will reveal that such a bound state shows a skin-mode-like photonic profile resulting from the nontrivial point-gap topology, *dubbed hidden bound state* [S7, S8].

(i) When the emitter is coupled to the sublattice  $a$ , the photonic weight  $c_{\alpha,k}$  ( $\alpha = a, b$ ) in momentum space is obtained as

$$c_{k,a} = c_{e,a} g_k \left[ E_b + \frac{i\kappa}{2} - \frac{J_2^2 + \kappa J_2 e^{-ik}}{E_b + i\kappa/2} \right]^{-1}, \quad \text{and} \quad c_{k,b} = c_{e,a} g_k \left[ \frac{(E_b + i\kappa/2)^2}{\kappa + J_2 e^{ik}} - J_2 e^{-ik} \right]^{-1}, \quad (\text{S37})$$

where  $g_k = g e^{-ikj_0}$ . The real-space photonic profile can be obtained by the inverse Fourier transformation of Eq. (S37). This leads to

$$c_{j,a} = \frac{g c_{e,a} (E_b + \frac{i\kappa}{2})}{L} \sum_k \frac{e^{ik(j-j_0)}}{[(E_b + \frac{i\kappa}{2})^2 - J_2^2] - \kappa J_2 e^{-ik}} = \frac{g c_{e,a} (E_b + \frac{i\kappa}{2}) y_A}{2\pi i \kappa J_2} \oint_{|y|=1} dy \frac{y^{j-j_0}}{y - \eta}, \quad (\text{S38})$$

and

$$c_{j,b} = \frac{g c_{e,a}}{L} \sum_k \frac{(\kappa + J_2 e^{ik}) e^{ik(j-j_0)}}{[(E_b + \frac{i\kappa}{2})^2 - J_2^2] - \kappa J_2 e^{-ik}} = \frac{g c_{e,a} \eta}{2\pi i \kappa J_2} \oint_{|y|=1} dy \frac{\kappa y^{j-j_0} + J_2 y^{j-j_0+1}}{y - \eta}, \quad (\text{S39})$$

where  $\eta = (\kappa J_2)/[(E_b + i\kappa/2)^2 - J_2^2]$ .

We consider the  $E_b$  lies inside the loop of the point-gap spectrum with  $|\kappa J_2| > |J_2^2 - (E_b + i\kappa/2)^2|$ . According to Eqs. (S38) and (S39), we obtain the real-space photonic profile as

$$c_{j,a} = \begin{cases} 0, & j \geq j_0, \\ -\frac{g c_{e,a} (E_b + i\kappa/2) \eta^{j-j_0+1}}{\kappa J_2}, & j < j_0, \end{cases} \quad (\text{S40})$$

and

$$c_{j,b} = \begin{cases} 0, & j \geq j_0, \\ -\frac{g c_{e,a}}{J_2}, & j = j_0 - 1, \\ -\frac{g c_{e,a} \eta^{j-j_0+1}}{J_2} - \frac{g c_{e,a} \eta^{j-j_0+2}}{\kappa}, & j < j_0 - 1. \end{cases} \quad (\text{S41})$$

(ii) When the emitter is coupled to the sublattice  $b$ , the photonic weight  $c_{\alpha,k}$  ( $\alpha = a, b$ ) in momentum space is obtained as

$$c_{k,a} = \frac{g c_{e,b} J_2 e^{-ik}}{(E_b + \frac{i\kappa}{2})^2 - J_2^2 - \kappa J_2}, \quad \text{and} \quad c_{k,b} = \frac{g c_{e,b} (E_b + \frac{i\kappa}{2})}{(E_b + \frac{i\kappa}{2})^2 - J_2^2 - \kappa J_2}. \quad (\text{S42})$$

The real-space photonic profile is obtained by the inverse Fourier transformation of Eq. (S42). This leads to

$$c_{j,a} = \frac{g c_{e,b} J_2}{L} \sum_k \frac{e^{ik(j-j_0-1)}}{(E_b + \frac{i\kappa}{2})^2 - J_2^2 - \kappa J_2 e^{-ik}} = \frac{g c_{e,b} \eta}{2\pi i \kappa} \oint_{|y|=1} dy \frac{y^{j-j_0-1}}{y - \eta}, \quad (\text{S43})$$

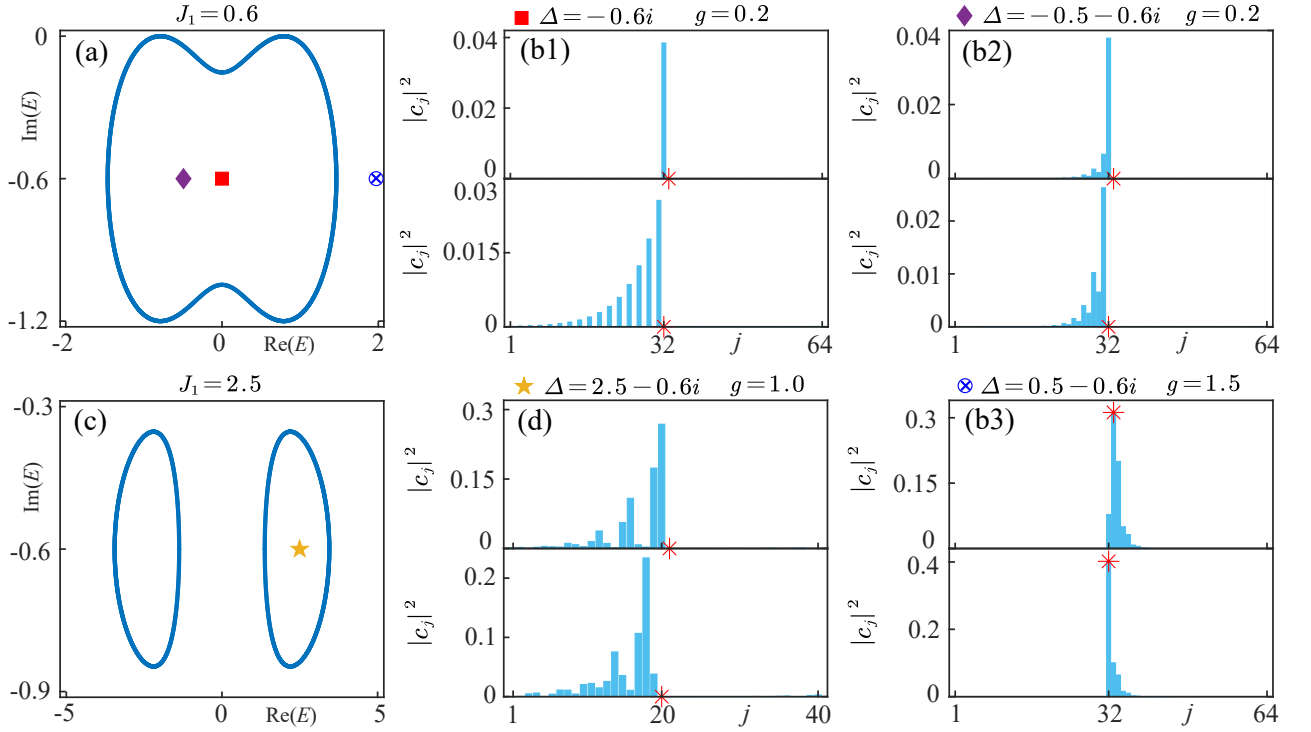


FIG. S2. Single-excitation point-gap spectrum (blue loops) of the bath under PBCs (a) for  $J_1 = 2.5$ , and (c) for  $J_1 = 0.6$ . The markers denote the eigenenergies of the bound states of a single emitter coupled to the bath for different  $\Delta$ . The corresponding site-resolved photon weights  $|c_j|^2$  are shown in (b1-b3) and (d), where the emitter is coupled to the sublattice  $a$  (b), denoted by the red asterisk, for the top (bottom) plot. The other parameters used are  $\kappa = 1.2$  and  $J_2 = 1.0$ .

and

$$c_{j,b} = \frac{g c_{e,b}(E_b + \frac{i\kappa}{2})}{L} \sum_k \frac{e^{ik(j-j_0)}}{(E_b + \frac{i\kappa}{2})^2 - J_2^2 - \kappa J_2 e^{-ik}} = \frac{g c_{e,b}(E_b + \frac{i\kappa}{2})\eta}{2\pi i \kappa J_2} \oint_{|y|=1} dy \frac{y^{j-j_0}}{y - \eta}, \quad (\text{S44})$$

$E_b$  lies inside the loop of the point-gap spectrum with  $|\kappa J_2| > |J_2^2 - (E_b + i\kappa/2)^2|$ , according to Eqs. (S43) and (S44), we obtain the real-space photonic profile as

$$c_{j,a} = \begin{cases} 0, & j > j_0, \\ -\frac{g c_{e,b} \eta^{(j-j_0)}}{\kappa}, & j \leq j_0, \end{cases} \quad (\text{S45})$$

and

$$c_{j,b} = \begin{cases} 0, & j \geq j_0, \\ -\frac{g c_{e,b}(E_b + \frac{i\kappa}{2})\eta^{(j-j_0+1)}}{\kappa J_2}, & j < j_0. \end{cases} \quad (\text{S46})$$

The above analytical results show that the bound state, with its eigenenergy lying inside the point gap, has its eigenstate located on only the left side of the emitter, no matter if the emitter is coupled to the sublattice  $a$  or  $b$ . Such a bound state behaves like the skin modes. Figure S2(a,b1,b2) plot the bound states and site-resolved photon weight for  $J_1 = \kappa/2$ . In spite of the detuning  $\Delta$ , the eigenstates are located on only the left side of the emitter due to the NHSE. While, outside the loop of the point gap, the bound state behaves like the conventional Hermitian bound states [see Figure S2(b3)]. In addition, in spite of the coexistence of point gap and line gap, bound states inside the point gap behave like skin modes, as shown in Fig. S2(c,d)

### C. Atomic weight

The atomic weight can be directly solved out using Eq. (S25). To have a simple form of the analytical solution for the bound-state wavefunction in Eq. (S25), we solve out the bound state for  $J_1 = \kappa/2$ . When the emitter is coupled

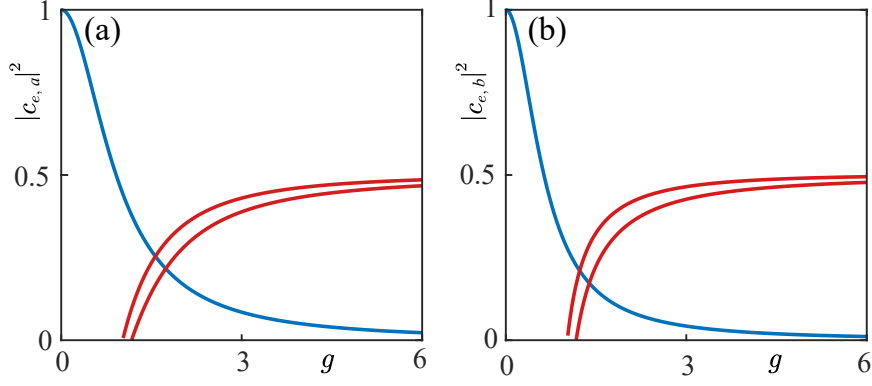


FIG. S3. Dependence of the atomic weights  $|c_{e,a}|$  and  $|c_{e,b}|$  of the hidden (blue curves) and Hermitian-like (red curves) bound states on the coupling strength  $g$  under PBCs for  $J_1 = \kappa/2$ , where the emitter is coupled to the sublattice  $a$  or  $b$ . The parameters used are  $\Delta = 0.2 - 0.4i$  and  $J_2 = 1.0$ .

to the sublattice  $a$ , the photonic weight reads

$$|c_{e,a}|^2 = \left[ 1 + \frac{4g^2}{w} + \frac{g^2(4J_2\kappa z_+^2 + u_a z_+ + 4J_2\kappa)}{4J_2\kappa v z_+(z_+ - z_-)} \theta(1 - |z_+|) + \frac{g^2(4J_2^2\kappa z_-^2 + u_a z_- + 4J_2\kappa)}{4J_2\kappa v z_-(z_- - z_+)} \theta(1 - |z_-|) \right]^{-1}, \quad (\text{S47})$$

where

$$u_a = 4J_2^2 - 2iE_b\kappa + 5\kappa^2 + 4|E_b|^2 + 2i\kappa E_b^*, \quad (\text{S48})$$

$$w = 4J_2^2 + \kappa^2 + 4i\kappa E_b^* - 4(E_b^*)^2, \quad \text{and} \quad v = J_2^2 - \left( E_b + \frac{i\kappa}{2} \right)^2, \quad (\text{S49})$$

$$p = 4J_2^2\kappa^2 + vw, \quad \text{and} \quad z_{\pm} = \frac{-p \pm \sqrt{p^2 - 16J_2^2\kappa^2vw}}{8J_2\kappa v}. \quad (\text{S50})$$

When the emitter is coupled to the sublattice  $b$ , the photonic weight reads

$$|c_{e,b}|^2 = \left[ 1 + \frac{g^2 u_b}{4J_2\kappa v(z_+ - z_-)} \theta(1 - |z_+|) + \frac{g^2 u_b}{4J_2\kappa v(z_- - z_+)} \theta(1 - |z_-|) \right]^{-1}, \quad (\text{S51})$$

where

$$u_b = 4J_2^2 - 2iE_b\kappa + \kappa^2 + 4|E_b|^2 + 2i\kappa E_b^*. \quad (\text{S52})$$

In Fig. S3, we calculate the dependence of the atomic weights  $|c_{e,a}|$  and  $|c_{e,b}|$  of the hidden (blue curves) and Hermitian-like (red curves) bound states on the coupling strength  $g$  under PBCs for  $J_1 = \kappa/2$ , where the emitter is coupled to the sublattice  $a$  or  $b$ . The emergence of hidden bound states with eigenenergies inside the point gap does not rely on the coupling strength  $g$ . In contrast, the conventional bound states with energies outside the point gap only appear for sufficiently large  $g$  [see also Fig. S2(a,b1-b3)].

#### IV. Effects of disorder on chiral and extended photon-emitter dressed states

The chiral-extended photon-emitter dressed state has the topological origin, and it is thus robust against the disorder. To illustrate this, we investigate the effect of two types of disorder: (a) the random cavity frequencies with the addition of the diagonal terms to the original Hamiltonian  $\hat{\mathcal{H}}_{\text{eff}} \rightarrow \hat{\mathcal{H}}_{\text{eff}} + \hat{\mathcal{H}}_{\text{diag}}$ , and (b) the random intercell hopping between

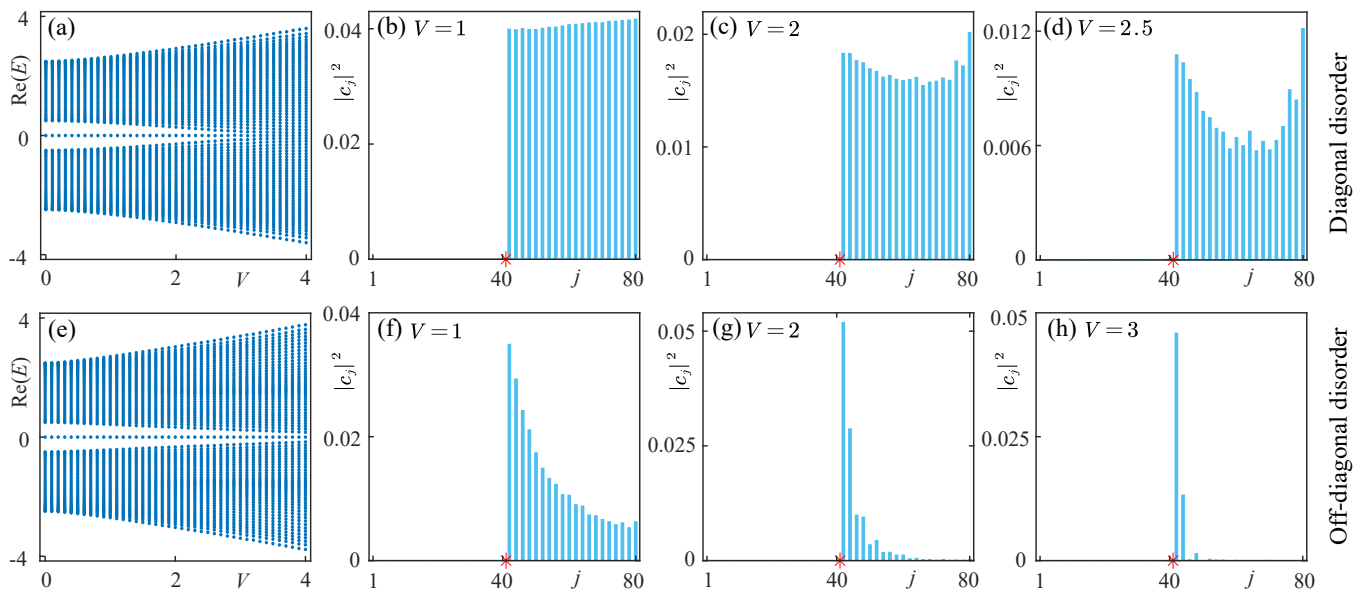


FIG. S4. Real part of the complex eigenspectrum  $E$  and the corresponding site-resolved photon weights  $|c_j|^2$  at the transition point  $J_2 = J_1 - \kappa/2$  under OBCs as a function of the disorder strength  $V$ , where a single emitter is coupled to the sublattice  $a$  of the disordered bath. The in-gap modes are the dressed photon-emitter state. (a-d) Disorder is applied to the cavity frequencies (diagonal disorder), and (e-h) the disorder is applied to the intercell couplings between cavities (off-diagonal disorder). The results are averaged over 1000 random realizations. The other parameters used are  $\Delta = -0.6i$ ,  $g = 0.5$ ,  $\kappa = 1.2$ ,  $J_1 = 1.6$ ,  $J_2 = 1.0$  and  $L = 40$ .

cavities with the addition of the off-diagonal terms to the original Hamiltonian  $\hat{\mathcal{H}}_{\text{eff}} \rightarrow \hat{\mathcal{H}}_{\text{eff}} + \hat{\mathcal{H}}_{\text{off}}$ . The Hamiltonians  $\hat{\mathcal{H}}_{\text{diag}}$  and  $\hat{\mathcal{H}}_{\text{off}}$  are written as

$$\hat{\mathcal{H}}_{\text{diag}} = \sum_{j=1}^L \left( \varepsilon_{a,j} \hat{a}_j^\dagger \hat{a}_j + \varepsilon_{b,j} \hat{b}_j^\dagger \hat{b}_j \right), \quad (\text{S53})$$

and

$$\hat{\mathcal{H}}_{\text{off}} = \sum_{j=1}^{L-1} \left( \varepsilon_{1,j} \hat{b}_j^\dagger \hat{a}_{j+1} + \text{H.c.} \right), \quad (\text{S54})$$

where  $\varepsilon_{a,j}$ ,  $\varepsilon_{b,j}$  and  $\varepsilon_{1,j}$  are taken from a uniform distribution within the range  $[-V/2, V/2]$  with the disorder strength  $V$ .

We consider a single emitter coupled to the sublattice  $a$  of the disordered SSH bath. Figure S4(a-d) plots the complex eigenspectrum  $E$  and the corresponding site-resolved photon weights  $|c_j|^2$  for the random cavity frequencies (diagonal disorder). The chirality of the in-gap dressed photon-emitter state and its corresponding extended photon profile remain quite robust against the disorder even for the strong disorder. For the random hopping between cavities (off-diagonal disorder), the chirality of the dressed state is still robust against the strong disorder, as shown in Fig. S4(e-h). While, the extended photon profile becomes localized for the ultrastrong disorder [see Fig. S4(g,h)].

## V. Effects of unequal emitter and cavity decay on chiral-extended photon-emitter dressed states

In the main text, we discuss the chiral-extended photon-emitter dressed states for  $\gamma = \kappa$ , where the photon weight at each  $b$  site is the same for the zero photon-emitter frequency detuning with  $\Delta_0 = 0$  [see also the top plot of Fig. S5(e)]. We now study the effects of the emitter decay rate  $\gamma$  on the mode distribution of the dressed state with  $\Delta_0 = 0$  and  $J_2 = J_1 - \kappa/2$ . As shown in Fig. S5, we show the site-resolved photon weights  $|c_j|^2$  for the emitter coupled to the sublattice  $a$  ( $b$ ) in the top (bottom) plot.

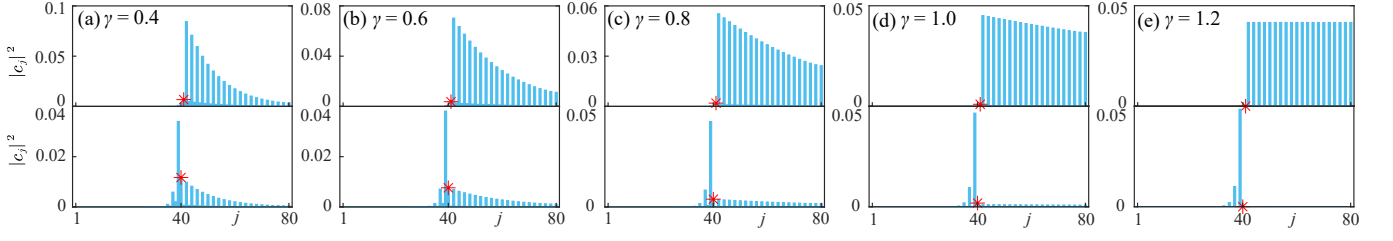


FIG. S5. Site-resolved photon weights  $|c_j|^2$  at transition point  $J_2 = J_1 - \kappa/2$  for (a)  $\gamma = 0.4$ , (b)  $\gamma = 0.6$ , (c)  $\gamma = 0.8$ , (d)  $\gamma = 1.0$ , and (e)  $\gamma = 1.2$  under OBCs. The emitter is coupled to the sublattice  $a$  ( $b$ ) for the top (bottom) plot. The other parameters used are  $g = 0.5$ ,  $\kappa = 1.2$ ,  $J_1 = 1.6$ ,  $J_2 = 1.0$  and  $L = 40$ .

## VI. Analytical solution of chiral-extended photon-emitter dressed states

### A. Single Emitter

We now consider a single emitter coupled to the sublattice  $\alpha \in \{a, b\}$  of the unit cell  $j_0$ . In the single-excitation subspace, spanned by  $\{|e\rangle|\text{vac}\rangle, |g\rangle|j, a\rangle, |g\rangle|j, b\rangle\}$  with  $j \in [1, L]$ , and under the open boundary condition (OBC), the Hamiltonian of the photon-emitter hybrid system is written as

$$\mathcal{H}_\alpha = \begin{pmatrix} \Delta & V_\alpha \\ V_\alpha^\dagger & H_p \end{pmatrix}, \quad (\text{S55})$$

where  $\alpha = a, b$ , indicating the sublattice  $a$  or  $b$  to which the emitter is coupled, the coupling vector

$$V_\alpha = (0, 0, 0, 0, \dots, g\delta_{\alpha,a}, g\delta_{\alpha,a}, 0, 0, \dots, 0), \quad (\text{S56})$$

and the Hamiltonian matrix of the SSH chain  $H_p$  becomes

$$H_p = \begin{pmatrix} -i\frac{\kappa}{2} & J_1 - \frac{\kappa}{2} & 0 & 0 & \cdots & 0 & 0 \\ J_1 + \frac{\kappa}{2} & -i\frac{\kappa}{2} & J_2 & 0 & \cdots & 0 & 0 \\ 0 & J_2 & -i\frac{\kappa}{2} & J_1 - \frac{\kappa}{2} & \cdots & 0 & 0 \\ 0 & 0 & J_1 + \frac{\kappa}{2} & -i\frac{\kappa}{2} & \cdots & 0 & 0 \\ \vdots & \vdots & \vdots & \vdots & \vdots & \vdots & \vdots \\ 0 & 0 & 0 & 0 & \cdots & -i\frac{\kappa}{2} & J_1 - \frac{\kappa}{2} \\ 0 & 0 & 0 & 0 & \cdots & J_1 + \frac{\kappa}{2} & -i\frac{\kappa}{2} \end{pmatrix}. \quad (\text{S57})$$

We first discuss the emitter coupled to the sublattice  $\alpha = a$ . We implement a similarity transformation to the Hamiltonian  $\mathcal{H}_a$  in Eq. (S55) with

$$\bar{\mathcal{H}}_a = S_a^{-1} \mathcal{H}_a S_a, \quad (\text{S58})$$

where  $S_a$  is a diagonal matrix whose diagonal elements are

$$\{1, r^{-(j_0-1)}, r^{1-(j_0-1)}, r^{1-(j_0-1)}, r^{2-(j_0-1)}, \dots, r^{L-1-(j_0-1)}, r^{L-1-(j_0-1)}, r^{L-(j_0-1)}\}, \quad \text{with } r = \sqrt{\frac{J_1 + \frac{\kappa}{2}}{J_1 - \frac{\kappa}{2}}}. \quad (\text{S59})$$



Then, the  $\bar{\mathcal{H}}_a$  is written as

$$\bar{\mathcal{H}}_a = \begin{pmatrix} \Delta & V_a \\ V_a^\dagger & \bar{H}_p \end{pmatrix}, \quad (\text{S60})$$

where  $\bar{H}_p$  reads

$$\bar{H}_p = \begin{pmatrix} -i\frac{\kappa}{2} & \bar{J}_1 & 0 & 0 & \cdots & 0 & 0 \\ \bar{J}_1 & -i\frac{\kappa}{2} & J_2 & 0 & \cdots & 0 & 0 \\ 0 & J_2 & -i\frac{\kappa}{2} & \bar{J}_1 & \cdots & 0 & 0 \\ 0 & 0 & \bar{J}_1 & -i\frac{\kappa}{2} & \cdots & 0 & 0 \\ \vdots & \vdots & \vdots & \vdots & \vdots & \vdots & \vdots \\ 0 & 0 & 0 & 0 & \cdots & -i\frac{\kappa}{2} & \bar{J}_1 \\ 0 & 0 & 0 & 0 & \cdots & \bar{J}_1 & -i\frac{\kappa}{2} \end{pmatrix}, \quad (\text{S61})$$

with  $\bar{J}_1 = \sqrt{(J_1 - \kappa/2)(J_1 + \kappa/2)}$ . After the similarity transformation, the photon-emitter Hamiltonian  $\bar{\mathcal{H}}_a$  describes a Hermitian system subject to the uniform local dissipation with rate  $\kappa/2$ .

When the emitter is coupled to the sublattice  $\alpha = b$ , we can also implement a similarity transformation to the Hamiltonian  $\mathcal{H}_b$  in Eq. (S55) with

$$\bar{\mathcal{H}}_b = S_b^{-1} \mathcal{H}_b S_b, \quad (\text{S62})$$

where  $S_b$  is a diagonal matrix whose diagonal elements are

$$\{1, r^{-j_0}, r^{1-j_0}, r^{1-j_0}, r^{2-j_0}, \dots, r^{L-1-j_0}, r^{L-1-j_0}, r^{L-j_0}\}. \quad (\text{S63})$$

Then,  $\bar{\mathcal{H}}_b$  is written as

$$\bar{\mathcal{H}}_b = \begin{pmatrix} \Delta & V_b \\ V_b^\dagger & \bar{H}_p \end{pmatrix}, \quad (\text{S64})$$

After the similarity transformation, the photon-emitter Hamiltonian  $\bar{\mathcal{H}}_b$  also describes a Hermitian system subjected to the uniform local dissipation with rate  $\kappa/2$ .

According to the Hamiltonian  $\bar{\mathcal{H}}_a$  in Eq. (S60) or  $\bar{\mathcal{H}}_b$  in Eq. (S64), in the single-excitation subspace, spanned by  $\{|e\rangle|\text{vac}\rangle, |g\rangle|j, \bar{a}\rangle, |g\rangle|j, \bar{b}\rangle\}$  with the similarity-transformed basis  $|g\rangle|j, \bar{\alpha}\rangle$  ( $\bar{\alpha} = \bar{a}, \bar{b}$ ) and  $j \in [1, L]$ , the eigenequation for the photon-emitter dressed states reads

$$\bar{\mathcal{H}} |\bar{\psi}_\alpha\rangle = (\bar{\mathcal{H}}_0 + \bar{\mathcal{H}}_e + \bar{\mathcal{V}}_\alpha) |\bar{\psi}_\alpha\rangle = E |\bar{\psi}_\alpha\rangle, \quad (\text{S65})$$

with the eigenenergy of the dressed state being  $E_d = E - i\kappa/2$ , and

$$\bar{\mathcal{H}}_0 = \sum_{j=1}^L (\bar{J}_1 |j, \bar{b}\rangle \langle j, \bar{a}| + J_2 |j, \bar{b}\rangle \langle j+1, \bar{a}| + \text{H.c.}), \quad (\text{S66})$$

$$\bar{\mathcal{H}}_e = \Delta_0 |e\rangle \langle e|, \quad (\text{S67})$$

$$\bar{\mathcal{V}}_\alpha = g (|e\rangle \langle j_0, \bar{\alpha}| + |j_0, \bar{\alpha}\rangle \langle e|). \quad (\text{S68})$$

The Hermitian SSH Hamiltonian  $\bar{\mathcal{H}}_0$  for  $J_2 = J_1 - \kappa/2$  (topological trivial phase) under OBCs can be solved out as [S12]

$$\bar{\mathcal{H}}_0 = \sum_{m=1}^{2L} \varepsilon_m |\varphi_m\rangle \langle \varphi_m|, \quad (\text{S69})$$

where the eigenvalue reads

$$\varepsilon_m = (-1)^m \sqrt{2\bar{J}_1 J_2 \cos \theta_m + \bar{J}_1^2 + J_2^2}, \quad (\text{S70})$$

with  $\theta_m$  being a real number satisfying

$$\bar{J}_1 \sin[(L+1)\theta_m] + J_2 \sin[L\theta_m] = 0, \quad (\text{S71})$$

and the eigenvectors are

$$|\varphi_m\rangle = \frac{1}{\sqrt{\mathcal{N}_m}} \sum_{j=1}^L (\varphi_{m,a}(j) |j, \bar{a}\rangle + \varphi_{m,b}(j) |j, \bar{b}\rangle). \quad (\text{S72})$$

Here,  $\mathcal{N}_m$  is the normalized constant for  $|\varphi_m\rangle$ , and the amplitudes  $\varphi_{m,a}(j)$  and  $\varphi_{m,b}(j)$  are given by [S12]

$$\varphi_{m,a}(j) = \sin[j\theta_m] + \frac{J_2}{\bar{J}_1} \sin[(j-1)\theta_m], \quad (\text{S73})$$

$$\varphi_{m,b}(j) = \frac{\varepsilon_m}{\bar{J}_1} \sin[j\theta_m]. \quad (\text{S74})$$

Utilizing the eigenvector  $\{|\varphi_m\rangle\}$ , we rewrite the Hamiltonian  $\bar{\mathcal{V}}_\alpha$  in Eq. (S68) as

$$\begin{aligned} \bar{\mathcal{V}}_\alpha &= g \left( \sum_{m=1}^{2L} |e\rangle \langle j_0, \bar{\alpha} | \varphi_m \rangle \langle \varphi_m | + \text{H.c.} \right), \\ &= g \left( \sum_{m=1}^{2L} \frac{\varphi_{m,\alpha}(j_0)}{\sqrt{\mathcal{N}_m}} |e\rangle \langle \varphi_m | + \text{H.c.} \right). \end{aligned} \quad (\text{S75})$$

Therefore, in the single-excitation subspace, spanned by  $\{|e\rangle |\text{vac}\rangle, |g\rangle |\varphi_m\rangle\}$  with  $m \in [1, 2L]$ , we would like to consider the dressed state

$$|\bar{\psi}_\alpha\rangle = \sum_{m=1}^{2L} \bar{c}_m |g\rangle |\varphi_m\rangle + \bar{c}_e |e\rangle |\text{vac}\rangle, \quad (\text{S76})$$

that satisfies the eigenequation in Eq. (S65) with total Hamiltonian  $\bar{\mathcal{H}}$  in the new basis  $\{|\varphi_m\rangle\}$ . Then we obtain

$$\varepsilon_m \bar{c}_m + \frac{g\varphi_{m,\alpha}^*(j_0)\bar{c}_e}{\sqrt{\mathcal{N}_m}} = E\bar{c}_m, \quad \forall m, \quad (\text{S77})$$

$$g \sum_{m=1}^{2L} \frac{\varphi_{m,\alpha}(j_0)\bar{c}_m}{\sqrt{\mathcal{N}_m}} + \Delta_0 \bar{c}_e = E\bar{c}_e. \quad (\text{S78})$$

According to Eq. (S77), the photon profile of the dressed state can be given by

$$\bar{c}_m = \frac{g\varphi_{m,\alpha}^*(j_0)}{\sqrt{\mathcal{N}_m}(E - \varepsilon_m)} \bar{c}_e, \quad (\text{S79})$$

where the atom profile  $\bar{c}_e$  can be determined by the normalization of the dressed state as

$$|\bar{c}_e|^2 = \left[ 1 + \sum_{m=1}^{2L} \frac{g^2 |\varphi_{m,\alpha}(j_0)|^2}{(E - \varepsilon_m)(E^* - \varepsilon_m^*) \mathcal{N}_m} \right]^{-1}. \quad (\text{S80})$$

Inserting Eq. (S79) into Eq. (S78) to eliminate  $\bar{c}_m$  yields

$$\left[ E - \Delta_0 - g^2 \sum_{m=1}^{2L} \frac{|\varphi_{m,\alpha}(j_0)|^2}{(E - \varepsilon_m) \mathcal{N}_m} \right] \bar{c}_e = 0. \quad (\text{S81})$$

According to Eqs. (S79)-(S81), we can solve  $E$ ,  $\bar{c}_m$ , and  $\bar{c}_e$ . Then, at the basis  $\{|e\rangle|\text{vac}\rangle, |g\rangle|j,a\rangle, |g\rangle|j,b\rangle\}$ , we obtain the wavefunction of the dressed state  $\psi_\alpha = S_\alpha \bar{\psi}_\alpha$ , where

$$\bar{\psi}_\alpha = [\bar{c}_e, \phi_1, \phi_2, \dots, \phi_m, \dots, \phi_{2L}]^T, \quad \text{with } \phi_m = \langle g, \varphi_m | \bar{\psi}_\alpha \rangle. \quad (\text{S82})$$

## B. Two Emitters

We now consider two emitters ( $|g_1\rangle, |e_1\rangle$ ) and ( $|g_2\rangle, |e_2\rangle$ ) coupled to site  $(\alpha_1, j_1)$  and  $(\alpha_2, j_2)$  of the same SSH bath, respectively. In this subsection, we focus on the situation when the atom-photon interaction strength between both emitters and the SSH bath is set as  $g_1 = g_2 = g$ . In the single-excitation subspace, spanned by  $\{|e_1\rangle|\text{vac}\rangle, |e_2\rangle|\text{vac}\rangle, |g\rangle|j,a\rangle, |g\rangle|j,b\rangle\}$  with  $j \in [1, L]$ , and under OBCs, the system Hamiltonian reads

$$\mathcal{H}_{\alpha_1\alpha_2} = \begin{pmatrix} \Delta & 0 & V_{\alpha_1} \\ 0 & \Delta & V_{\alpha_2} \\ V_{\alpha_1}^\dagger & V_{\alpha_2}^\dagger & H_p \end{pmatrix}. \quad (\text{S83})$$

Then the eigenequation for the photon-emitter dressed states becomes

$$\mathcal{H}|\Psi_{\alpha_1\alpha_2}\rangle = (\mathcal{H}_p + \mathcal{H}_{e_1} + \mathcal{H}_{e_2} + \mathcal{V}_{\alpha_1\alpha_2})|\Psi_{\alpha_1\alpha_2}\rangle = E_d|\Psi_{\alpha_1\alpha_2}\rangle, \quad (\text{S84})$$

with the eigenenergy of the dressed state being  $E_d$ , and

$$\begin{aligned} \mathcal{H}_p &= \sum_{j=1}^L \left[ \left( J_1 + \frac{\kappa}{2} \right) |j,b\rangle \langle j,a| + \left( J_1 - \frac{\kappa}{2} \right) |j,a\rangle \langle j,b| \right] \\ &+ \sum_{j=1}^{L-1} (J_2 |j,b\rangle \langle j+1,a| + J_2 |j+1,a\rangle \langle j,b|) \\ &- \sum_{j=1}^L \frac{i\kappa}{2} (|j,a\rangle \langle j,a| + |j,b\rangle \langle j,b|), \end{aligned} \quad (\text{S85})$$

$$\mathcal{H}_e = \mathcal{H}_{e_1} + \mathcal{H}_{e_2} = \Delta (|e_1\rangle \langle e_1| + |e_2\rangle \langle e_2|), \quad (\text{S86})$$

$$\mathcal{V}_{\alpha_1\alpha_2} = g(|e_1\rangle \langle j_1, \alpha_1| + |j_1, \alpha_1\rangle \langle e_1|) + g(|e_2\rangle \langle j_2, \alpha_2| + |j_2, \alpha_2\rangle \langle e_2|). \quad (\text{S87})$$

Due to the non-Hermiticity of the bath Hamiltonian  $\mathcal{H}_p$  in Eq. (S85), the right and left eigenstates of  $\mathcal{H}_p$  can be defined as

$$\mathcal{H}_p |\varphi_m^R\rangle = E |\varphi_m^R\rangle, \quad \mathcal{H}_p^\dagger |\varphi_m^L\rangle = E^* |\varphi_m^L\rangle, \quad (\text{S88})$$

whose biorthogonal conditions and completeness conditions are given by  $\langle \varphi_m^R | \varphi_n^L \rangle = \langle \varphi_m^L | \varphi_n^R \rangle = \delta_{mn}$  and  $\sum_m |\varphi_m^L\rangle \langle \varphi_m^R| = \sum_m |\varphi_m^R\rangle \langle \varphi_m^L| = 1$ , respectively. Using these relations, the bath Hamiltonian  $\mathcal{H}_p$  can be expressed in terms of quasi-particle energy bands as

$$\mathcal{H}_p = \sum_{m=1}^{2L} \left( \varepsilon_m - \frac{i\kappa}{2} \right) |\varphi_m^R\rangle \langle \varphi_m^L|, \quad (\text{S89})$$

and the right and left eigenvectors are given by

$$|\varphi_m^R\rangle = \frac{1}{\sqrt{\bar{\mathcal{N}}_m}} \sum_{j=1}^L (\varphi_{m,a}^R(j) |j, a\rangle + \varphi_{m,b}^R(j) |j, b\rangle), \quad (\text{S90})$$

$$|\varphi_m^L\rangle = \frac{1}{\sqrt{\bar{\mathcal{N}}_m}} \sum_{j=1}^L (\varphi_{m,a}^L(j) |j, a\rangle + \varphi_{m,b}^L(j) |j, b\rangle). \quad (\text{S91})$$

Here,  $\bar{\mathcal{N}}_m$  is the normalized constant in the biorthogonal condition. By utilizing the inverse of the similarity transformation to Eqs. (S73) and (S74), the amplitudes of  $\varphi_{m,a}^{R/L}(j)$  and  $\varphi_{m,b}^{R/L}(j)$  are given by

$$\varphi_{m,a}^R(j) = \left( \frac{J_1 + \kappa/2}{J_1 - \kappa/2} \right)^{\frac{j}{2}} (\sin[j\theta_m] + \frac{J_2}{J_1} \sin[(j-1)\theta_m]), \quad (\text{S92})$$

$$\varphi_{m,b}^R(j) = \frac{\varepsilon_m}{J_1 - \kappa/2} \left( \frac{J_1 + \kappa/2}{J_1 - \kappa/2} \right)^{\frac{j}{2}} \sin[j\theta_m], \quad (\text{S93})$$

$$\varphi_{m,a}^L(j) = \left( \frac{J_1 - \kappa/2}{J_1 + \kappa/2} \right)^{\frac{j}{2}} (\sin[j\theta_m] + \frac{J_2}{J_1} \sin[(j-1)\theta_m]), \quad (\text{S94})$$

$$\varphi_{m,b}^L(j) = \frac{\varepsilon_m}{J_1 + \kappa/2} \left( \frac{J_1 - \kappa/2}{J_1 + \kappa/2} \right)^{\frac{j}{2}} \sin[j\theta_m]. \quad (\text{S95})$$

Utilizing the completeness condition  $\sum_{m=1}^{2L} |\varphi_m^R\rangle \langle \varphi_m^L| = 1$ , we rewrite the atom-photon interaction Hamiltonian  $\mathcal{V}_{\alpha_1\alpha_2}$  in Eq. (S87) as

$$\begin{aligned} \mathcal{V}_{\alpha_1\alpha_2} = & g \left( \sum_{m=1}^{2L} \frac{\varphi_{m,\alpha_1}^R(j_1)}{\sqrt{\bar{\mathcal{N}}_m}} |e_1\rangle \langle \varphi_m^L| + \sum_{m=1}^{2L} \frac{[\varphi_{m,\alpha_1}^L(j_1)]^*}{\sqrt{\bar{\mathcal{N}}_m}} |\varphi_m^R\rangle \langle e_1| \right) \\ & + g \left( \sum_{m=1}^{2L} \frac{\varphi_{m,\alpha_2}^R(j_2)}{\sqrt{\bar{\mathcal{N}}_m}} |e_2\rangle \langle \varphi_m^L| + \sum_{m=1}^{2L} \frac{[\varphi_{m,\alpha_2}^L(j_2)]^*}{\sqrt{\bar{\mathcal{N}}_m}} |\varphi_m^R\rangle \langle e_2| \right). \end{aligned} \quad (\text{S96})$$

We employ the resolvent method to solve the evolution dynamics of two emitters coupled to the topological bath [S13, S14]. Using the Hamiltonian  $\mathcal{H} = \mathcal{H}_p + \mathcal{H}_{e_1} + \mathcal{H}_{e_2} + \mathcal{V}_{\alpha_1\alpha_2}$  in Eqs. (S86), (S89) and (S96), the resolvent operator of the whole system is defined as

$$\mathcal{G}(z) = \frac{1}{z - \mathcal{H}} = \frac{1}{z - \mathcal{H}_{pe} - \mathcal{V}_{\alpha_1\alpha_2}}, \quad (\text{S97})$$

where

$$\mathcal{H}_{pe} = \mathcal{H}_p + \mathcal{H}_{e_1} + \mathcal{H}_{e_2}. \quad (\text{S98})$$

We now consider the single-excitation spanned by the emitter and bath Hamiltonian  $\mathcal{H}_{pe}$ , which consists of the atomic excitation  $\{|e_1\rangle|\text{vac}\}, |e_2\rangle|\text{vac}\}$ , and the quasi-particle excitation  $\{|g\rangle|\varphi_m^R\rangle\}$  with  $m \in [1, 2L]$ . The photon-emitter interaction term  $\mathcal{V}_{\alpha_1\alpha_2}$  describes the coupling between the subspaces  $\{|e_1\rangle|\text{vac}\}, |e_2\rangle|\text{vac}\}$  and  $\{|g\rangle|\varphi_m^R\rangle\}$ . In the following, we use the following notations  $|e_1\rangle := |e_1\rangle|\text{vac}\}$ ,  $|e_2\rangle := |e_2\rangle|\text{vac}\}$  and  $|\varphi_m^R\rangle := |g\rangle|\varphi_m^R\rangle$  for convenience. Then, we define the projector operator

$$\mathcal{P} = |e_1\rangle \langle e_1| + |e_2\rangle \langle e_2|, \quad (\text{S99})$$

and its complementary

$$\mathcal{Q} = \sum_{m=1}^{2L} |\varphi_m^R\rangle \langle \varphi_m^L|. \quad (\text{S100})$$

Therefore, the constrained propagator  $\mathcal{G}_p(z)$  is written as

$$\mathcal{G}_p(z) \equiv \mathcal{P}\mathcal{G}(z)\mathcal{P}. \quad (\text{S101})$$

Starting from  $(z - \mathcal{H})\mathcal{G}(z) = \mathbf{1}$ , and manipulating it on the right by  $\mathcal{P}$  and on the left by  $\mathcal{P}$  or  $\mathcal{Q}$ , the constrained propagator can be derived as

$$\mathcal{G}_p(z) = \frac{\mathcal{P}}{z - \mathcal{P}\mathcal{H}_{pe}\mathcal{P} - \mathcal{P}\Sigma(z)\mathcal{P}}, \quad (\text{S102})$$

where  $\Sigma(z)$  is called the level-shift operator [S13], defined as

$$\begin{aligned} \Sigma(z) &= \mathcal{V}_{\alpha_1\alpha_2} + \mathcal{V}_{\alpha_1\alpha_2} \frac{\mathcal{Q}}{z - \mathcal{Q}\mathcal{H}_{pe}\mathcal{Q} - \mathcal{Q}\mathcal{V}_{\alpha_1\alpha_2}\mathcal{Q}} \mathcal{V}_{\alpha_1\alpha_2}, \\ &= \mathcal{V}_{\alpha_1\alpha_2} + \mathcal{V}_{\alpha_1\alpha_2} \frac{\mathcal{Q}}{z - \mathcal{H}_p} \mathcal{V}_{\alpha_1\alpha_2}, \end{aligned} \quad (\text{S103})$$

with

$$\begin{aligned} \mathcal{V}_{\alpha_1\alpha_2} \frac{\mathcal{Q}}{z - \mathcal{H}_p} \mathcal{V}_{\alpha_1\alpha_2} &= \sum_{m=1}^{2L} \frac{g^2 \varphi_{m,\alpha_1}^R(j_1) [\varphi_{m,\alpha_1}^L(j_1)]^* / \bar{\mathcal{N}}_m}{z - \varepsilon_m + i\kappa/2} |e_1\rangle \langle e_1| \\ &\quad + \sum_{m=1}^{2L} \frac{g^2 \varphi_{m,\alpha_1}^R(j_1) [\varphi_{m,\alpha_2}^L(j_2)]^* / \bar{\mathcal{N}}_m}{z - \varepsilon_m + i\kappa/2} |e_1\rangle \langle e_2| \\ &\quad + \sum_{m=1}^{2L} \frac{g^2 \varphi_{m,\alpha_2}^R(j_2) [\varphi_{m,\alpha_1}^L(j_1)]^* / \bar{\mathcal{N}}_m}{z - \varepsilon_m + i\kappa/2} |e_2\rangle \langle e_1| \\ &\quad + \sum_{m=1}^{2L} \frac{g^2 \varphi_{m,\alpha_2}^R(j_2) [\varphi_{m,\alpha_2}^L(j_2)]^* / \bar{\mathcal{N}}_m}{z - \varepsilon_m + i\kappa/2} |e_2\rangle \langle e_2|. \end{aligned} \quad (\text{S104})$$

We now proceed to calculate the non-unitary real-time dynamics governed by  $|\psi_t\rangle = e^{-i\hat{\mathcal{H}}_{\text{eff}}t} |\psi_0\rangle$  for two emitters (labeled as 1 and 2) coupled to sites  $j_{1,\alpha_1}$  and  $j_{2,\alpha_2}$  ( $\alpha_1, \alpha_2 = a$  or  $b$ ) of the bath with  $j_{2,\alpha_2} > j_{1,\alpha_1}$ , respectively. The initial state is chosen as one excited emitter  $|e_1\rangle$  or  $|e_2\rangle$  with  $|\psi_0\rangle = |e_n\rangle |\text{vac}\rangle$  ( $n = 1$  or  $2$ ), and the time-evolved state can be expanded as

$$|\psi_t\rangle = \left( \sum_{m=1}^{2N} c_m(t) |\varphi_m^R\rangle \langle \text{vac}| + \sum_{n=1}^2 c_{e_n}(t) |e_n\rangle \langle g| \right) |gg\rangle \otimes |\text{vac}\rangle. \quad (\text{S105})$$

Then, the component  $\mathcal{P}|\psi_t\rangle$  can be evaluated by the resolvent method [S13] as

$$\mathcal{P}|\psi_t\rangle = \frac{i}{2\pi} \int_{-\infty}^{+\infty} dE \mathcal{G}_p(E + i0^+) e^{-iEt} |\psi_0\rangle. \quad (\text{S106})$$

Using Eq. (S106), we can express  $\mathbf{c}_e(t) = [c_{e_1}(t), c_{e_2}(t)]^T$  as

$$\mathbf{c}_e(t) = \frac{i}{2\pi} \int_{-\infty}^{+\infty} dE \mathcal{G}_p(E + i0^+) e^{-iEt} \mathbf{c}_e(0), \quad (\text{S107})$$

where, according to Eqs. (S102)-(S104), we explicitly write  $\mathcal{G}_p(z)$  as

$$\mathcal{G}_p(E) = \begin{pmatrix} \frac{1}{E - \Delta - \bar{\mathcal{T}}(\alpha_1, \alpha_1)} & \frac{1}{E - \mathcal{F}(\alpha_1, \alpha_2) \bar{\mathcal{T}}(\alpha_1, \alpha_2)} \\ \frac{1}{E - \mathcal{F}(\alpha_2, \alpha_1) \bar{\mathcal{T}}(\alpha_1, \alpha_2)} & \frac{1}{E - \Delta - \bar{\mathcal{T}}(\alpha_2, \alpha_2)} \end{pmatrix}, \quad (\text{S108})$$

where

$$\mathcal{T}(\alpha_1, \alpha_2) = g^2 \sum_{m=1}^{2L} \frac{\varphi_{m,\alpha_1}(j_{1,\alpha_1})\varphi_{m,\alpha_2}(j_{2,\alpha_2})}{(E - \varepsilon_m + i\kappa/2)\mathcal{N}_m}, \quad (\text{S109})$$

and

$$\mathcal{F}(\alpha_1, \alpha_2) = \left( \frac{J_1 + \kappa/2}{J_1 - \kappa/2} \right)^{\frac{\delta_{\alpha_1,b}}{2}} \left( \frac{J_1 - \kappa/2}{J_1 + \kappa/2} \right)^{\frac{\delta_{\alpha_2,b}}{2}} \left( \frac{J_1 + \kappa/2}{J_1 - \kappa/2} \right)^{\frac{j_{1,\alpha_1} - j_{2,\alpha_2}}{2}}. \quad (\text{S110})$$

We assume a small  $g$ , a large band gap of the topological bath under OBCs and  $\Delta = -i\kappa/2$ . According to Eqs. (S107)-(S110) and Eq. (S81), the main contribution from the diagonal elements of the Green function  $\mathcal{G}_p(z)$  to the time evolution is the dressed state for small  $g$  and  $\Delta = -i\kappa/2$ . The off-diagonal elements contribute to the state exchanges between two emitters. Remarkably, such state exchange is asymmetric [see Eq. (S110)]. To be specific, when the emitter at the site  $j_{2,\alpha_2}$  is initially excited, there is no excitation transferred to the emitter at site  $j_{1,\alpha_1}$  for the large distance  $|j_{1,\alpha_1} - j_{2,\alpha_2}|$  between them, due to the power-law decay of  $\mathcal{F}(\alpha_1, \alpha_2)$ .

---

\* These authors contributed equally

† E-mail: [liutao0716@scut.edu.cn](mailto:liutao0716@scut.edu.cn)

- [S1] M. O. Scully and M. S. Zubairy, *Quantum Optics* (Cambridge University Press, 1997).
- [S2] H. P. Breuer and F. Petruccione, *The Theory of Open Quantum Systems* (Oxford University Press, 2007).
- [S3] G. S. Agarwal, *Quantum Optics* (Cambridge University Press, 2012).
- [S4] D. A. Lidar, "Lecture notes on the theory of open quantum systems," arXiv:1902.00967 (2020).
- [S5] A. González-Tudela and J. I. Cirac, "Markovian and non-Markovian dynamics of quantum emitters coupled to two-dimensional structured reservoirs," *Phys. Rev. A* **96**, 043811 (2017).
- [S6] Z. Gong, S. Higashikawa, and M. Ueda, "Zeno Hall effect," *Phys. Rev. Lett.* **118**, 200401 (2017).
- [S7] Z. Gong, M. Bello, D. Malz, and F. K. Kunst, "Anomalous behaviors of quantum emitters in non-Hermitian baths," *Phys. Rev. Lett.* **129**, 223601 (2022).
- [S8] Z. Gong, M. Bello, D. Malz, and F. K. Kunst, "Bound states and photon emission in non-Hermitian nanophotonics," *Phys. Rev. A* **106**, 053517 (2022).
- [S9] S. Yao and Z. Wang, "Edge states and topological invariants of non-Hermitian systems," *Phys. Rev. Lett.* **121**, 086803 (2018).
- [S10] K. Yokomizo and S. Murakami, "Non-Bloch band theory of non-Hermitian systems," *Phys. Rev. Lett.* **123**, 066404 (2019).
- [S11] M. Bello, G. Platero, J. I. Cirac, and A. González-Tudela, "Unconventional quantum optics in topological waveguide QED," *Sci. Adv.* **5** (2019), 10.1126/sciadv.aaw0297.
- [S12] C.-X. Guo, C.-H. Liu, X.-M. Zhao, Y. Liu, and S. Chen, "Exact solution of non-Hermitian systems with generalized boundary conditions: Size-dependent boundary effect and fragility of the skin effect," *Phys. Rev. Lett.* **127**, 116801 (2021).
- [S13] C. Cohen-Tannoudji, J. Dupont-Roc, and G. Grynberg, *Atom-Photon Interactions: Basic Process and Applications* (John Wiley and Sons, 1998).
- [S14] E. N. Economou, *Green's Functions in Quantum Physics* (Springer Berlin Heidelberg, 2006).